Science & Technology Facilities Council

Wide Range Propagation Model

Report on Modelling of Rain Attenuation

11th December 2008

Table of Contents

Introduction 3
Weaknesses of current approaches 5
Not using the full rain distribution 5
Testing with the full rain rate distribution 7
The path reduction factor 9
Candidate WRPM rain models 12
The 2003 RAL model 12
Models proposed by the Peoples Republic of China 13
Model proposed by Brazil 15
Selection of a model for the WRPM 18
Rain and wet snow 19
UK Rain Statistics 20
Maximum possible rain rate. 22
Rain Time 24

Annex 1 – The P.530-12 Rain Model 33
2.4 Attenuation due to hydrometeors 33
2.4.1 Long-term statistics of rain attenuation 33
2.4.2 Combined method for rain and wet snow 34
2.4.3 Frequency scaling of long-term statistics of rain attenuation 36
2.4.4 Polarization scaling of long-term statistics of rain attenuation 36
2.4.5 Statistics of event duration and number of events 37
2.4.6 Rain attenuation in multiple hop networks 37
2.4.7 Prediction of outage due to precipitation 42

Annex 2 – The P618-9 Rain model 43
2.2 Attenuation by precipitation and clouds 43
2.2.1 Prediction of attenuation statistics for an average year 43

Introduction

The purpose of this document is to investigate a new rain attenuation model suitable for use in the Wide Range Propagation model. This work is part of work package WP1b: Attenuation effects—rain and atmospheric gases. The rain attenuation model will make use of the full rain rate distribution as available from measurements or maps. Current methods use only one point on the rain rate distribution to represent the whole path.

The proposed model is based on existing ITU-R methods where appropriate; this will help to gain acceptance within the ITU-R community. For reference, the current methods for terrestrial and earth space have been extracted from their associated recommendations and are shown Annex 1 – The P.530-12 Rain Model and in Annex 2 – The P618-9 Rain model.

It is important that the model is smooth, monotonic and applicable to all time percentages 0-100%. This is not quite as simple as it appears. Rain does not occur for much of the time, when there is no rain there is no rain attenuation. When rain does occur the rain rate will not be uniform along the entire path. Further at vanishingly small time percentages the rain rate can not be allowed to become infinite but must saturate at some value. We might expect the model to look something like Figure 1.

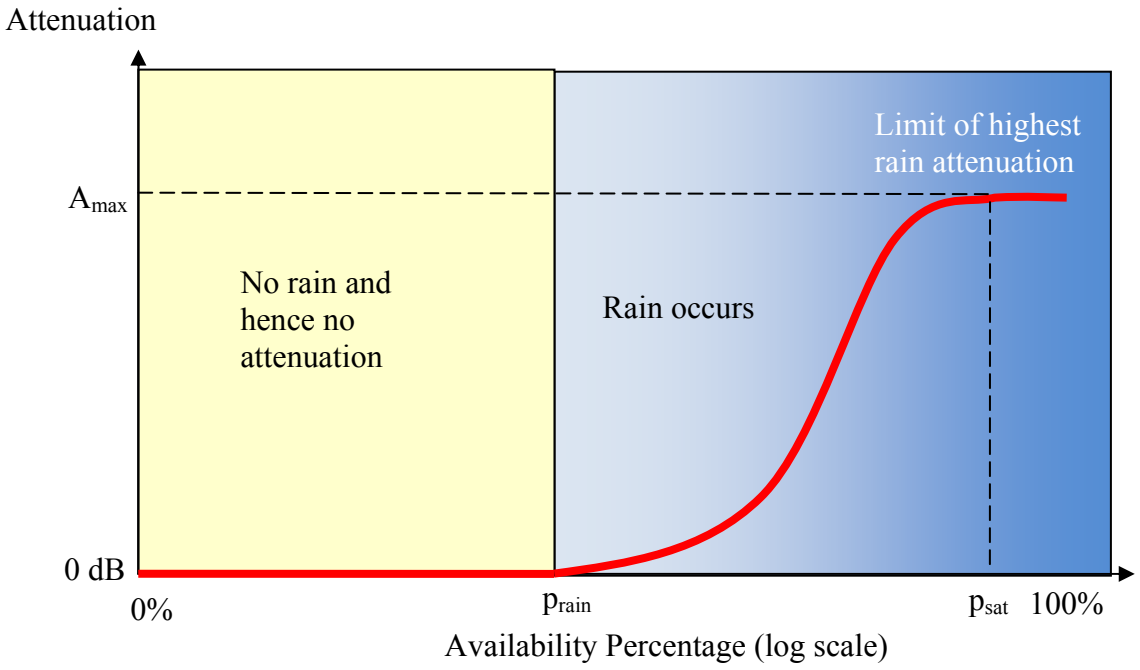

Figure 1 - Rain attenuation model

The time percentage below which rain does not occur at a specific location is p_{rain}, an estimate of which is available from ITU-R P.837-5. The maximum rain attenuation is A_{max}. We do not know what this maximum value is but clearly there must be some physical limit on the maximum rain rate. Both of these thresholds are functions of climate and link geometry. While it should be obvious that the attenuation will increase with the link length through rain, the probability of encountering rain along a path also rises with the path length, i.e. p_{rain} decreases as the link length

increases. The cumulative distribution function must by definition be monotonic[1]. Although ITU-R P.837-5 provides the probability of rain, currently ITU-R P.618-9 assumes rain in only present for 5% of the time and P530-12 is only valid for less than 1% of time.

It is worth briefly revisiting how these recommendations work out the rain attenuation. Both start by calculating the specific attenuation due to rain based on the relationship:

$$A_s = kR^{\alpha} \quad \text{dB/km} \tag{1}$$

Where R is the rainfall rate in mm/hr and k and α are tabulated constants that depend on frequency and polarisation. These constants are available in tabulated form and as a set of curve fits in Recommendation P.838-3. The tabulated constants were derived from theory, based on measured drop size and shape distributions and account for both the scattering and absorption of the microwave wave front. The curve fits were based on UK input 3J-18 2003 and are suitable for use in computer programmes implementing the method.

The overall attenuation is found by integrating the specific attenuation along the path.

$$A_{total} = \int_0^d A(x)\,.dx = \int_0^d kR(x)^{\alpha}.dx \tag{2}$$

The rain rate and hence the attenuation may vary significantly along longer paths and for practical use a path-average value is taken.

$$A_{total} = \int_0^d kR_{av}^{\alpha}.dx = d.kR_{av}^{\alpha} = d.A_{av} \tag{3}$$

In both P530-12 and in P618-9 this is achieved by assuming a constant rain rate, calculating the attenuation based on this rain rate and then applying an effective path length through rain.

$$A_{total} = d_{eff}.A_s \tag{4}$$

The effective path length is a complex function that differs between the two recommendations.

$$d_{eff} = d.F(A_s, d, p, f, \theta, \varphi \ldots.) \tag{5}$$

[1] For interpolated distributions, this will be true if the synthetic distribution is obtained by a linear interpolation of nearby measurements, so long as those measurements themselves are monotonic AND the interpolation function is not percentage time dependent.

Note that the rain rate is assumed constant and the path length through the rain is adjusted. It may be more appropriate to adjust the rain rate, though as in equation (1) the rain rate is raised to a power, a simple averaging function is likely to be inaccurate.

Weaknesses of current approaches

The values of k and α given in ITU-R P.838-3 are considered to be universally applicable. It is important to note that that this is a gross approximation, one that has been tested to give good results in the UK at the 99.99% availability level, which corresponds to rain rates of around 20-30mm/hr. In practice both k and α vary considerably with the type of rain, specifically the drop sizes[2] the drop shapes and orientation relative to the plane of polarisation and with the temperature of the rain.

In developing the tables of k and α given in P.838-3 a standard distribution of drop sizes, shapes, orientations and temperatures was assumed. We need to be careful when attempting to extend the model to use the full rain rate distribution as this distribution will be a function of the rain rate and the local climate.

Not using the full rain distribution

P.530-12 and P618-9 only make use of the 0.01% rain rate not exceeded value[3]. A recent modification to the rain rate maps given ITU-R P837-5 makes available the complete distribution of rain rate. In theory, to make use of the full rain rate distribution, a simple replacement of the specific attenuation equations[4] should be sufficient, but in practice this may not be advisable. The appropriate equations are shown in Figure 2 for P618-9 and Figure 3 for P530-12.

If $p \geq 1\%$ or $|\varphi| \geq 36°$: $\beta = 0$

If $p < 1\%$ and $|\varphi| < 36°$ and $\theta \geq 25°$: $\beta = -0.005(|\varphi| - 36)$

Otherwise: $\beta = -0.005(|\varphi| - 36) + 1.8 - 4.25 \sin\theta$

$$A_p = A_{0.01}\left(\frac{p}{0.01}\right)^{-(0.655 + 0.033 \ln(p) - 0.045 \ln(A_{0.01}) - \beta(1-p)\sin\theta)} \quad \text{dB}$$

Figure 2 - Time percentage scaling in P618-9, valid for 0.001% to 5% time.

$$\frac{A_p}{A_{0.01}} = 0.12\, p^{-(0.546 + 0.043 \log_{10} p)}$$

$$\frac{A_p}{A_{0.01}} = 0.07\, p^{-(0.855 + 0.139 \log_{10} p)}$$

[2] The drop size distribution is particularly important as the scattering cross section is proportional to the sixth power of the drop diameter whereas the drop volume is proportional to the cube of the diameter. The same rain rate may have very different scattering characteristics depending on the ratio of large and small drops.

[3] Note one has to take care to use the correct definition of time percentage, the rain rate exceeded for 0.01% rain rate is used in calculating the 99.99% availability margin.

[4] Equations 35,36 in P530-12 and 7,8 in P618-9

Paths above 30 degrees latitude Paths below 30 degrees latitude.

Figure 3 - Time percentage scaling in P530-12, valid for 0.001% to 1% time.

A few calculations will demonstrate these methods are only very approximately equivalent. Our latitude in the UK is always above 36 degrees so the β calculation and the θ elevation angle correction in P618-9 do not apply. It is the specific attenuation that is scaled, not the rain rate and this implies a frequency dependence of the rain structure. This is non-physical but probably compensates to some extent for differing drop size distributions.

The P530-12 scaling is demonstrated in Figure 4. The factor is only a function of latitude and probability and has an unfortunate discontinuity at 30^{o} latitude.

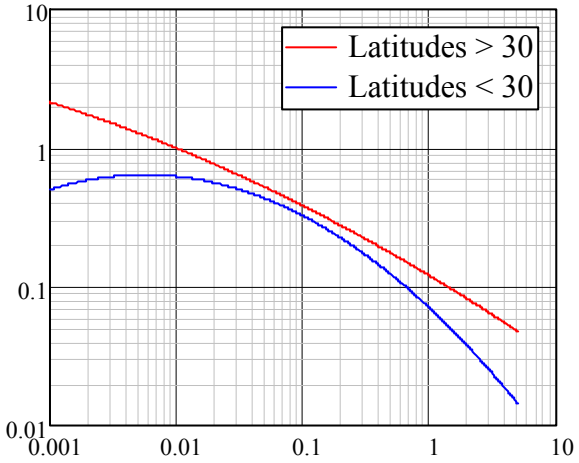

Figure 4 – Ratio $A_p/A_{0.01}$ for P530 above and below 30 degrees latitude

The P618-9 scaling factor is a function of the specific attenuation as demonstrated by equation 6. Figure 5 shows the P618-9 scaling for selected specific attenuations and time percentages.

$$\frac{A_p}{A_{0.01}} = \left(\frac{p}{0.01}\right)^{-[0.655+0.033\ln(p)-0.045\ln(A_{0.01})]} \quad \text{dB/km} \tag{6}$$

The P618-9 method is taking into account differing drop size distributions and the effects of the melting layer; simply substituting the rain rate in place of the given method may not work as expected. The two methods agree at 0.01% as long as the latitude is greater than 35^{0}. The most likely reason for the different approaches is that satellite links always have to pass through the melting layer. Until recently P.530 ignored the melting layer and the effects of sleet and snow. The latest version of P530-12 now includes in section 2.4.2, a combined rain and wet snow model.

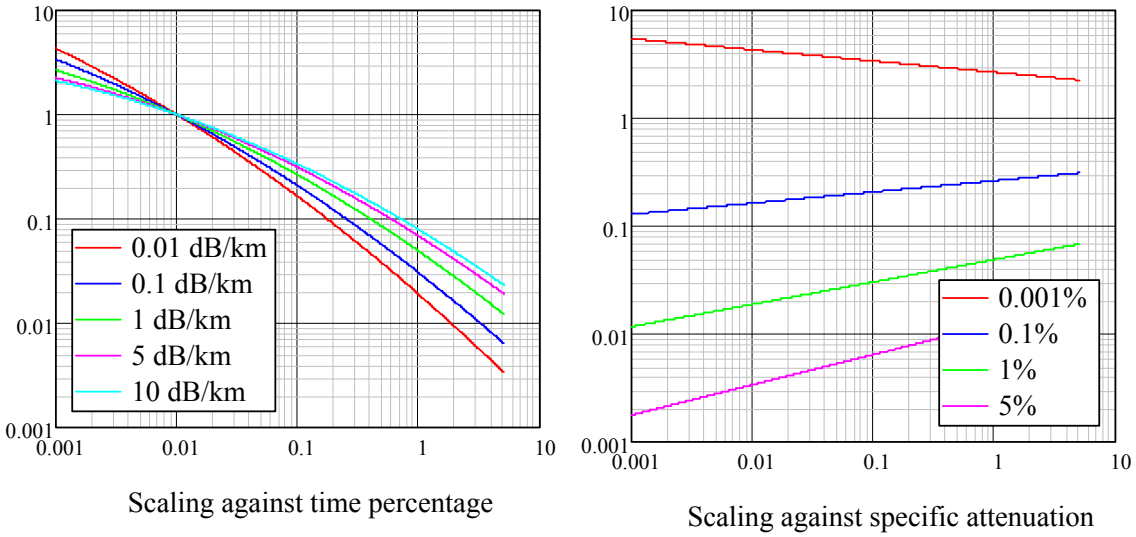

Figure 5 – Ratio $A_p/A_{0.01}$ for P618 at 52N

Testing with the full rain rate distribution

A new method was proposed to the ITU-R by RAL in 2005 for satellite links. This is based on the full rainfall rate distribution and agrees well with measurements. This method also considers the effects of clouds and the melting layer; while this is appropriate for satellite links it is not yet appropriate for terrestrial links. We need to evaluate if further development of this model is needed.

The specific attenuation calculation specified in ITU-R P.530-12 will be used with the modification that the full rain rate distribution is substituted in calculating the specific attenuation to determine if a correction is necessary.

Figure 6 shows some measured UK rain rate distributions. Both log and linear rain rate axes are given, the log-log plot tends to hide the importance of the variability of the rain rate but does demonstrate the power law fit. Possibly the only certain conclusion that can be made from these distributions is that there is considerable variability. However, a trend appears to be present and is shown by the red line, which joins the average rain rate at each time percentage. A trend line has been added based on a simple power law.

The power law, $R = 3.25p^{-0.4}$ allows us to generate a "typical" UK distribution. While this hides the true variability of the distributions it is useful in testing the P530 attenuation model.

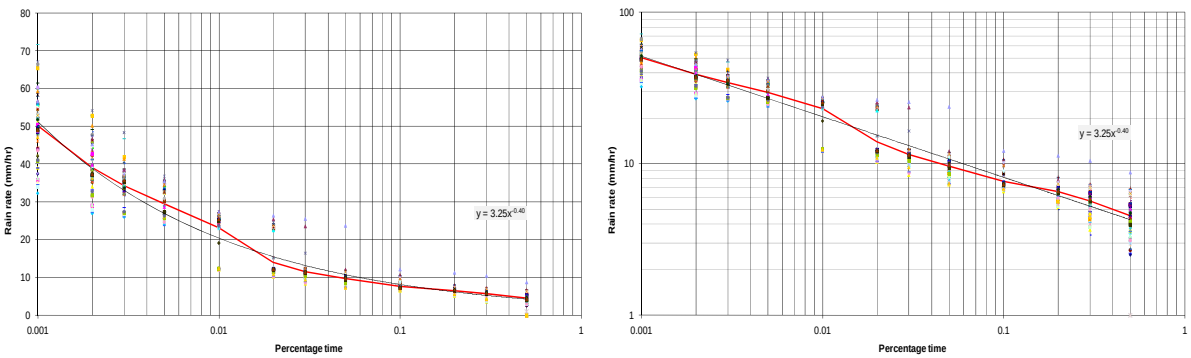

Figure 6 – Rain rate distributions (UK Data)

A selection of the specific attenuation constants k and α are shown in Table 1. The subscripts h and v represent horizontal and vertical polarisation respectively. The figure for 23 GHz has been highlighted and surrounding values included because the lack of a peak in k or α here demonstrates that water vapour attenuation is not folded into the rain attenuation model. There has been some uncertainty expressed over this point. Figure 7 illustrates graphically the specific attenuation against rain rate using the model for horizontal polarisation.

Frequency (GHz)	k_H	α_H	k_V	α_V
1	0.0000259	0.9691	0.0000308	0.8592
3	0.0001390	1.2322	0.0001942	1.0688
5	0.0002162	1.6969	0.0002428	1.5317
7	0.001915	1.4810	0.001425	1.4745
10	0.01217	1.2571	0.01129	1.2156
12	0.02386	1.1825	0.02455	1.1216
15	0.04481	1.1233	0.05008	1.0440
20	0.09164	1.0568	0.09611	0.9847
22	0.1155	1.0329	0.1170	0.9700
23	0.1286	1.0214	0.1284	0.9630
24	0.1425	1.0101	0.1404	0.9561
25	0.1571	0.9991	0.1533	0.9491
30	0.2403	0.9485	0.2291	0.9129
35	0.3374	0.9047	0.3224	0.8761
40	0.4431	0.8673	0.4274	0.8421
45	0.5521	0.8355	0.5375	0.8123
50	0.6600	0.8084	0.6472	0.7871

Table 1 - Selected k and α from P838-3

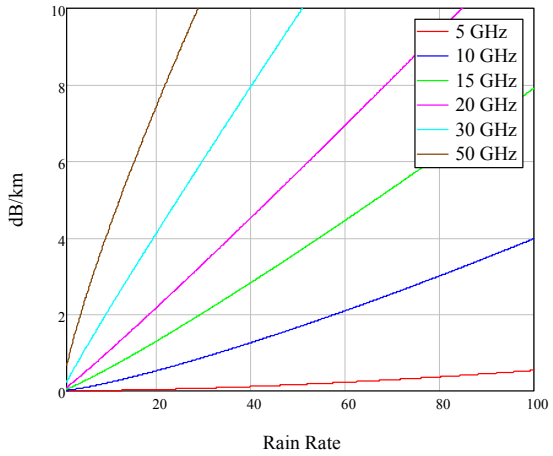

Figure 7 – Specific attenuations based on rain rate and kα

Figure 8 shows the difference in specific attenuation that results from using the rain rate distribution, as modelled for the UK and the method in P.530-12. Both graphs are based on a 0.01% rain rate of 20mm/hr which is reasonable for the UK. The differences are shown in Figure 9 and have become significant at 0.001%. The error at 10 GHz appears to be 50% and is 120% at 5 GHz, though it hardly matters as the attenuation is so low at 5GHz.

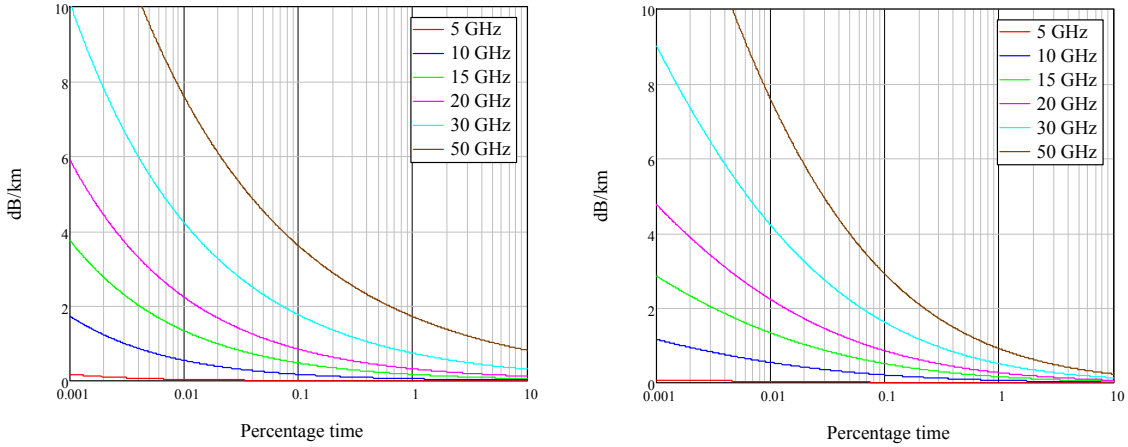

Figure 8 – Specific attenuations based on rain rate distribution and P530-12

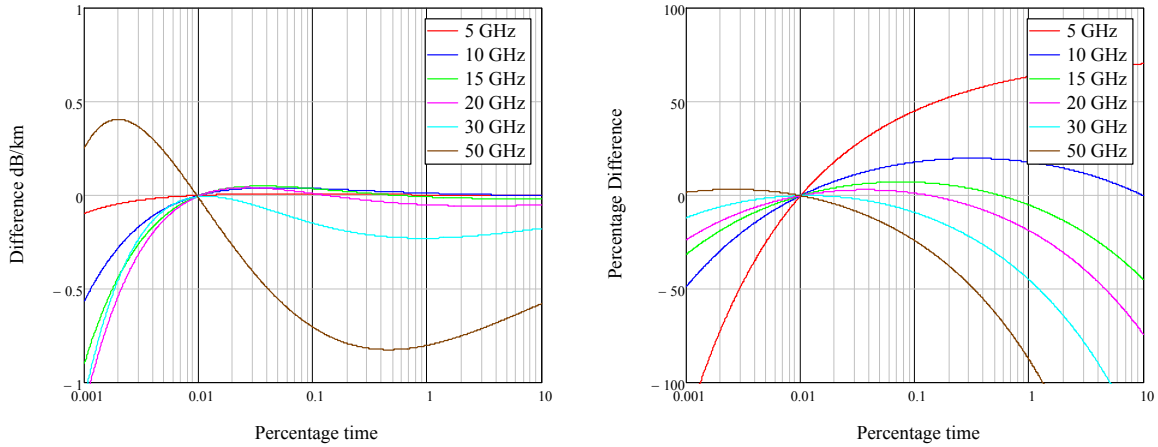

Figure 9 – Differences (P530-12 – Rain Rate based)

These differences arise because we are comparing two models, both of which may be an over-simplification of reality. However it does demonstrate that it is probably not appropriate to simply substitute the rain rate distribution into P.530-12.

The path reduction factor

The specific attenuation due to rain must be integrated along the entire path. The approach used by the current ITU-R recommendations (see equations 4 and 5), is to use a path reduction factor, that

reduces the effective path length and hence the predicted attenuation for longer paths in recognition of this non-uniformity.

It is only appropriate to consider the P530-12 model as the model in P618-9 only expects to work over short ranges; even at low elevation angles, the path will raise above the rain within 10-20km.

The P530-12 path reduction factor is based on the 0.01% rain rate, R_{001}.

$$r = \frac{1}{1 + d / d_0} \tag{7}$$

where d is the path length and:

$$d_0 = 35\ e^{-0.015\ R_{0.01}} \tag{8}$$

d_o is valid for areas where R_{001} is below 100mm/hr, which includes all of the UK. If R_{001} is above 100mm/hr, the 100mm/hr value should be used. The link attenuation is found by multiplying the specific attenuation by this reduced path length.

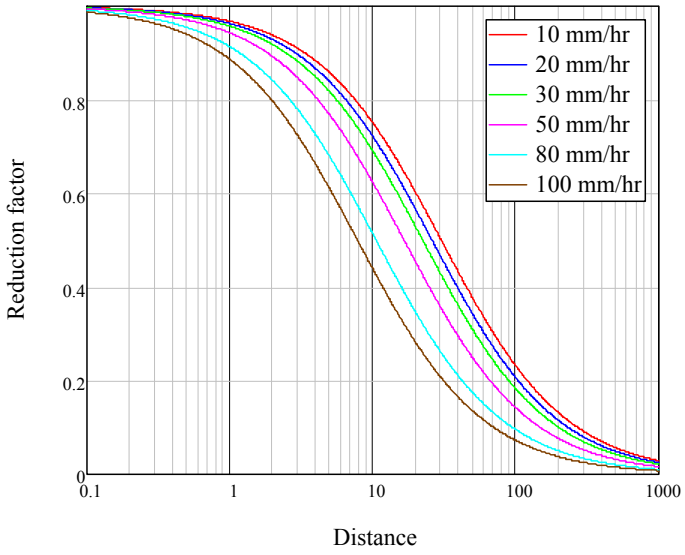

Figure 10 – Path reduction factor from P530-12

Although we do not intend to use it, it is interesting to note that the method used in P618 to calculate the horizontal path reduction factor, while also based on the specific attenuation at 0.01% time, includes an explicit frequency dependence:

$$r = \frac{1}{1 + 0.78\sqrt{\frac{dkR_{0.01}^{\alpha}}{f}} - 0.38(1 - e^{-2d})} \tag{9}$$

Figure 11 shows some results applying the P618-9 horizontal path reduction factor.

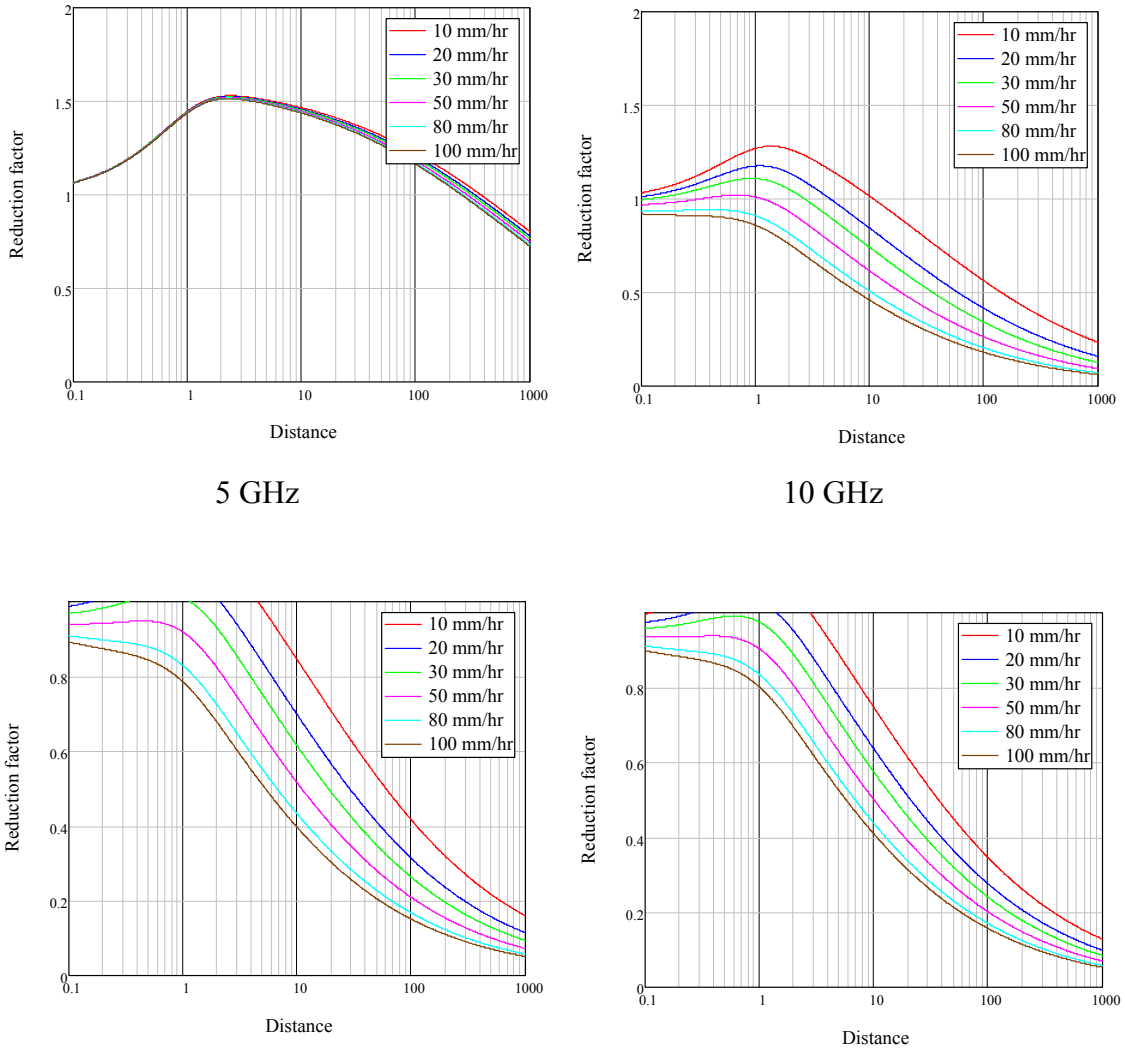

Figure 11 – Path reduction factors from P618-9

The question arises, should the full rain rate distribution be used in calculating the path reduction factor? There are arguments on both sides and the answer is probably that it should be; however P530-12 makes no attempt to do this. The issue is more complex and using only the rain rate distribution may not be sufficient. The local climate, specifically the incidence of stratiform and convective rain and link orientation with respect to the predominant wind direction may be important. This requires further investigation.

Candidate WRPM rain models

Several replacements for the model given in P.530-12 have been proposed within the ITU-R. We will now look at the most promising of these. The intention is to handle the issue of the 0-100% applicability by constraining the rain rate distribution to cover 0-100%. We do not therefore need to worry about this aspect in the rain attenuation model

The 2003 RAL model

A new model including the path length adjustment factor was proposed by the UK in 2003 in document 3J-16. As in P.530-12 and P.618-9 this takes the form:

$$A = kR^{\alpha} d \cdot r(R, d) \tag{10}$$

Where d is the path length, in km, and $r(R,d)$ is the path length reduction factor, a function of rainfall rate, R and path length. The difference to P.530-12 is the use of the rain distribution rather than $R_{0.01}$ and the format of the reduction function:

$$r = \frac{1}{0.874 + 0.0255(R^{0.54} - 1.7)d^{0.7}} \tag{11}$$

Figure 12 shows the value of the function given in equation 11 and the difference between the new method and P530-12 is shown in Figure 13. This model is extensively tested against data in 3J-16 and in general gives superior results.

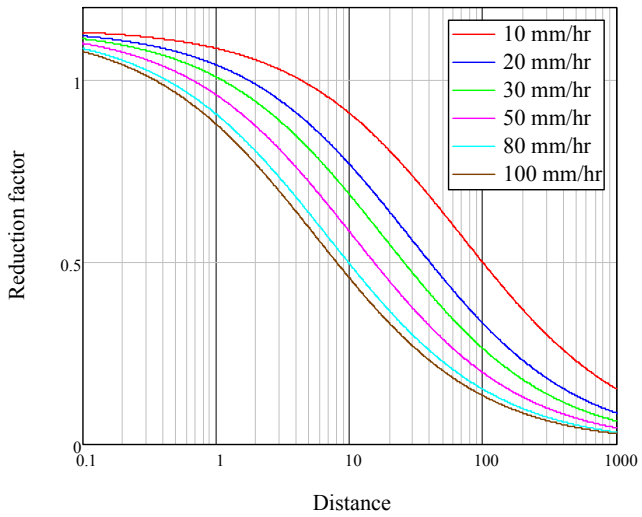

Figure 12 – UK 2003 path reduction factor

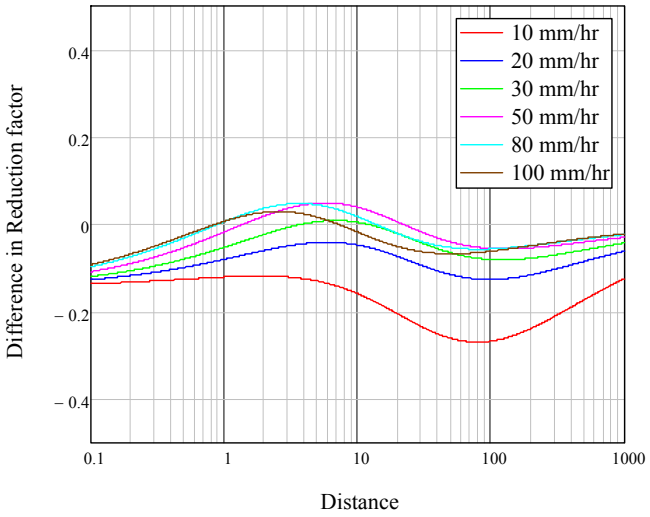

Figure 13 – P530-12 – UK 2003 proposed path reduction factors

While this model does not take account of differing climates it does meet our requirement to work over the full rain rate distribution.

Models proposed by the Peoples Republic of China

The Peoples Republic of China proposed a model in document 3J96 2005. While this was shown to be an improvement against the measurement database at 0.01% time it does not cover the complete time percentage range. This model was of the form:

$$r = \frac{1}{0.477 d^{0.633} R_{0.01}^{0.073\alpha} f^{0.123} - 10.579(1 - e^{-0.024d})} \tag{12}$$

$$A_p = A_{0.01}\left[\frac{p}{0.01}\right]^{-\left[0.864-0.026\ln\left(\frac{1+p}{p}\right)-0.022\ln(1+A_{0.01})-0.08\ln(f)-0.226(1+p)\right]} \quad (13)$$

3J53 – 2005 contains a useful set of comparisons of this and alternative models, including that from the UK. China further developed their path length reduction factor model in 3J20 2008, based on an EXCELL rain model.

$$r = \frac{1}{0.19k^{-0.052}R_0^{0.31\alpha} - 1.7k^{0.68\alpha}R_0^{0.48\alpha}d^{0.48}\left(e^{-0.92R_0^{-0.057}d^{0.48}} - 0.5\right)} \quad (14)$$

Where R_0 is the rainfall rate measured at the transmitter.

The model assumes there is only one rain cell along the path with the constants in equation 14 being found by a regression fit to the database. This fits well against the ITU-R measurement databank using the ITU-R testing variable. It is not made entirely clear in 3J20 2008, but it is assumed that the full rain rate distribution is used for calculating the rain attenuation rather than equation 13. An analysis of equation 14 is presented in Figure 14. From this it appears the path reduction factor behaves very strangely for short paths. This strange behaviour rules this model out from further consideration.

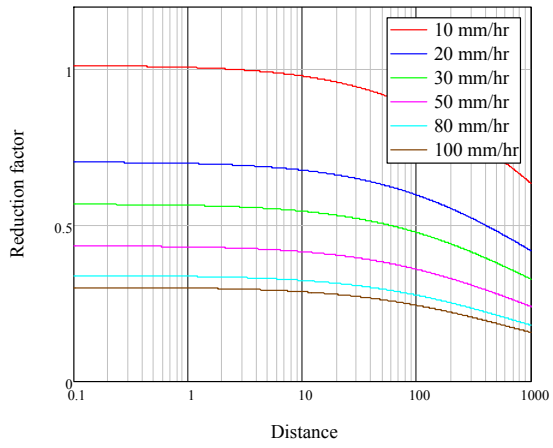

5 GHz

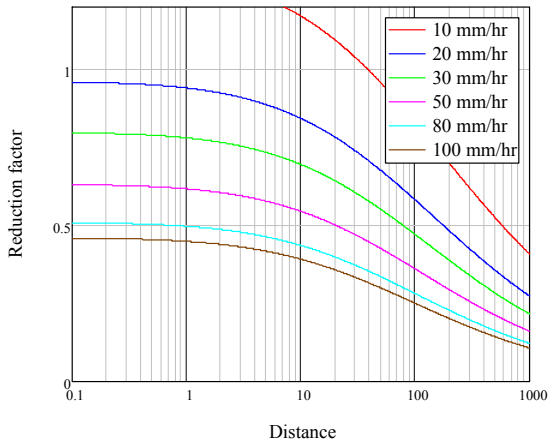

7 GHz

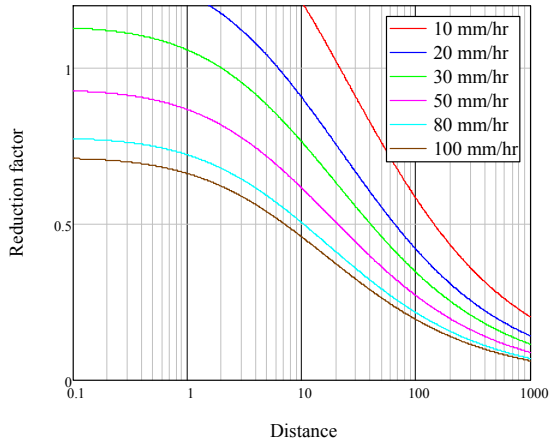

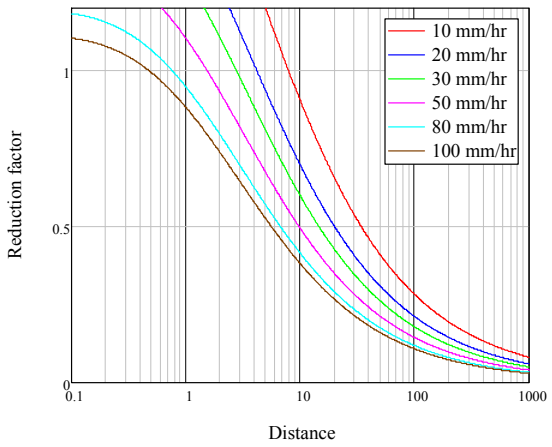

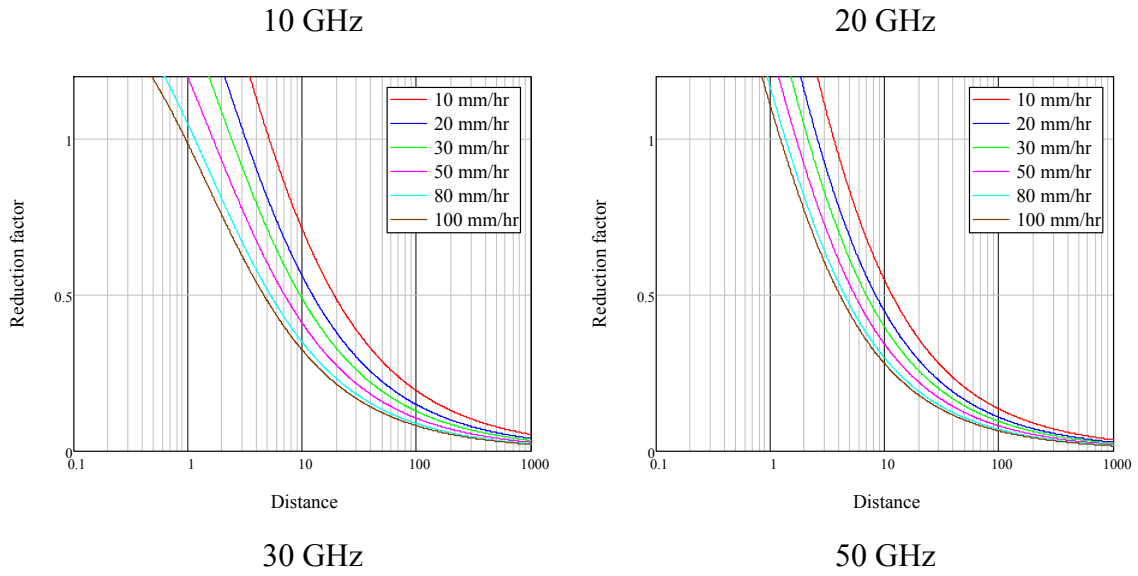

Figure 14 – China 2008 path reduction factor

Model proposed by Brazil

Brazil, in document 3J23 2008 provide a new model which does use the whole distribution. It introduces the concept of an effective rain rate which applies to the whole path and depends on the path length which is used in addition to a path reduction factor.

$$A_p = k\left[1.763\,R^{0.753+0.197/L_S\cos\theta}\right]^{\alpha}\frac{d}{1+\dfrac{d}{119R^{-0.244}}} \qquad (15)$$

Where θ is the elevation angle and the other terms have their usual definitions. This model has been tested against the ITU-R databank and appears to give good results. A comparison was made with the UK model and the models proposed by Australia and China based on the standard test variable for rain attenuation given in Recommendation ITU-R P.311-12.

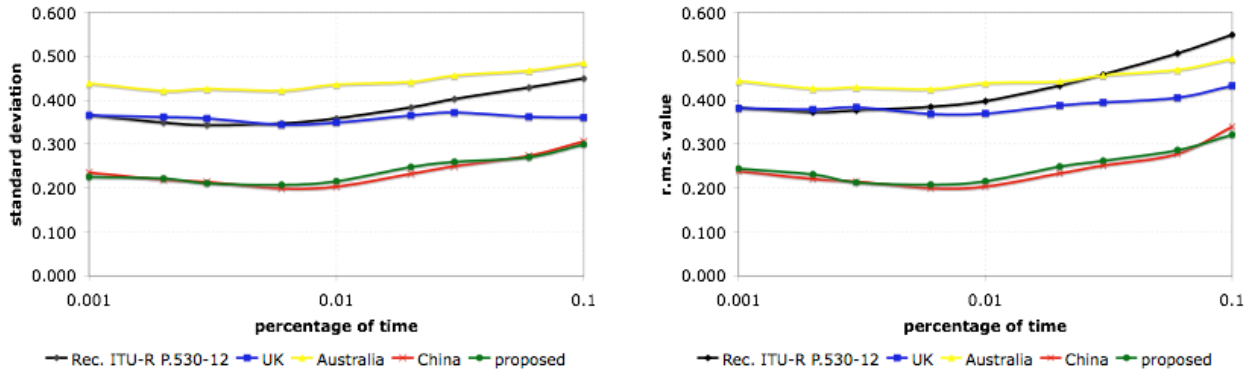

Figure 15 – Testing of Brazil model against terrestrial ITU-R database and other proposed models

This model is similar in form to the UK 2003 model, assuming a link elevation of zero degrees where equation 15 simplifies to:

$$A_p = k\left[1.763R_p^{0.753+0.197/d}\right]^{\alpha}\left(\frac{d}{1+\frac{d}{119R_p^{-0.244}}}\right) \qquad (16)$$

Effective rain rate term *Effective path length term*

It must be noted that the model from Brazil is not valid if d becomes small due to the 0.197/d term in the exponent of the effective rain rate.

This unfortunate behaviour is demonstrated by Figure 16. While 3J23 acknowledges that the effective rain rate should be allowed to be larger than 1, allowing it to approach infinity is not appropriate and it is suggested this model should not be used below 1km.

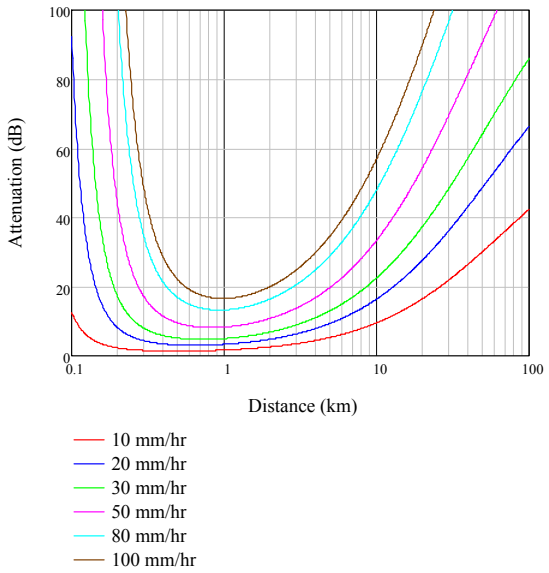

Figure 16 – Testing of Brazil model at 20GHz for Horizontal polarisation

The model from Brazil has a great advantage in being also applicable to satellite links where it takes the form:

$$A_p = k\left[1.763R^{0.753+0.197/L_S\cos\theta}\cos\theta + \frac{203.6}{L_S^{2.455}}R^{0.354+0.088/L_S\cos\theta}\sin\theta\right]^{\alpha}\frac{L_S}{1+\frac{L_S\cos\theta}{119R^{-0.244}}} \qquad (17)$$

Where the term L_s in the slant path length as calculated in P618-9.

Again the results are promising though the improvement is small.

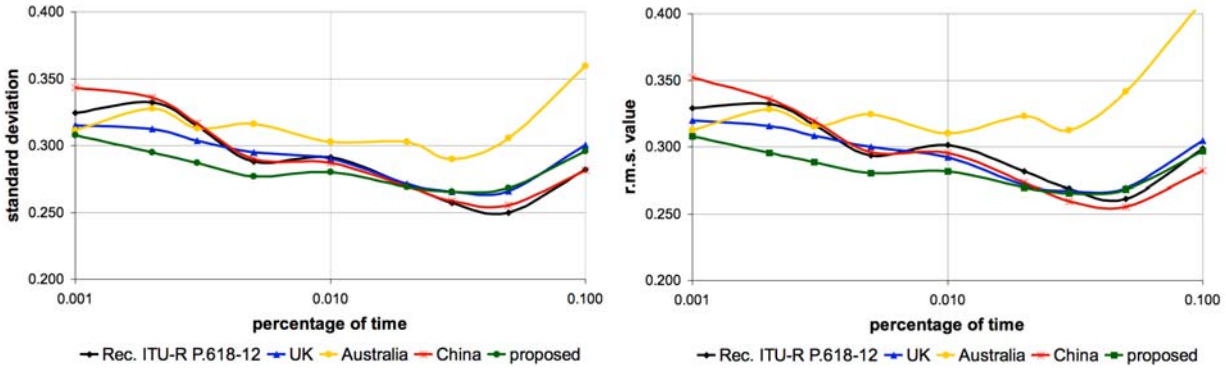

Figure 17 – Testing of Brazil model against ITU-R satellite database and other proposed models

Selection of a model for the WRPM

Owing to our need to use the full rain rate distribution, there are only three models considered appropriate, the UK model from 2003, The Chinese model from 2008 and the Brazilian model from 2007. The models will give very different results. The unusual performance of the Chinese model at low path lengths is unlikely to be acceptable. The model from Brazil also has a problem for very short links though less severe and correctable by limiting the reduction factor to the 1km value.

A comparison between the two models is shown in Figure 18. Compared to the UK model, the model from Brazil gives higher attenuation in the 10-100km range and lower attenuation beyond around 100km for rain rates above 20mm/h.

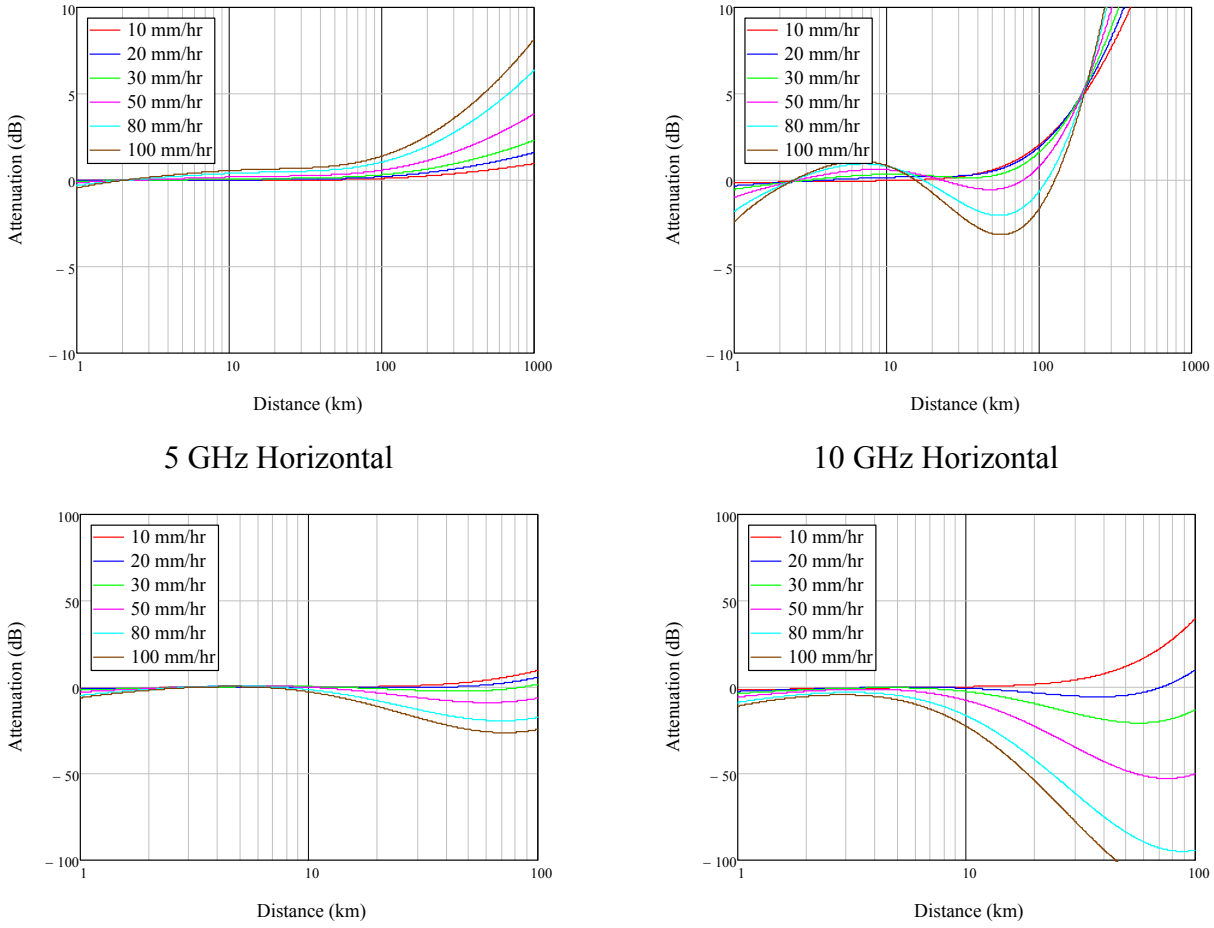

Figure 18 – Differences (UK 2003 Model – Brazil 2008 Model)

The model from Brazil does appear to give the best results against the measured data from the ITU-R – however that measured data does not include many long paths at higher frequencies nor many very short paths. Unfortunately choosing between the models based on the ITU-R data is difficult because:

a) there are few measurements of rain rate and rain attenuation distributions made together

b) of the measurement data sets, few are on longer paths at higher frequencies or on shorter paths at lower frequencies

We are unable to address point (a) with the new rain rate distributions given in recommendation P.837-5 as a proxy for rain rate measurements. An investigation of rain gauge data (Figure 6) shows that these do not agree well with rain rate measurements made in the UK. Point (b) matters because this is where the models differ most. The UK model is not too far from the existing model in ITU-R P.530-12, the models from Brazil and China are very different. The "safe" choice would be the UK model yet the comparison with data suggests the Brazilian model gives a better global result.

Rain and wet snow

Recommendation P530-12 has a model for including the effects of wet snow, or sleet and for links passing through the melting layer in clouds. Figure 19 demonstrates that the specific attenuation is higher in regions where there are melting particles. This leads to additional attenuation and a model was developed in the UK based on a method reported in 3M45 Annex 9, 2004.

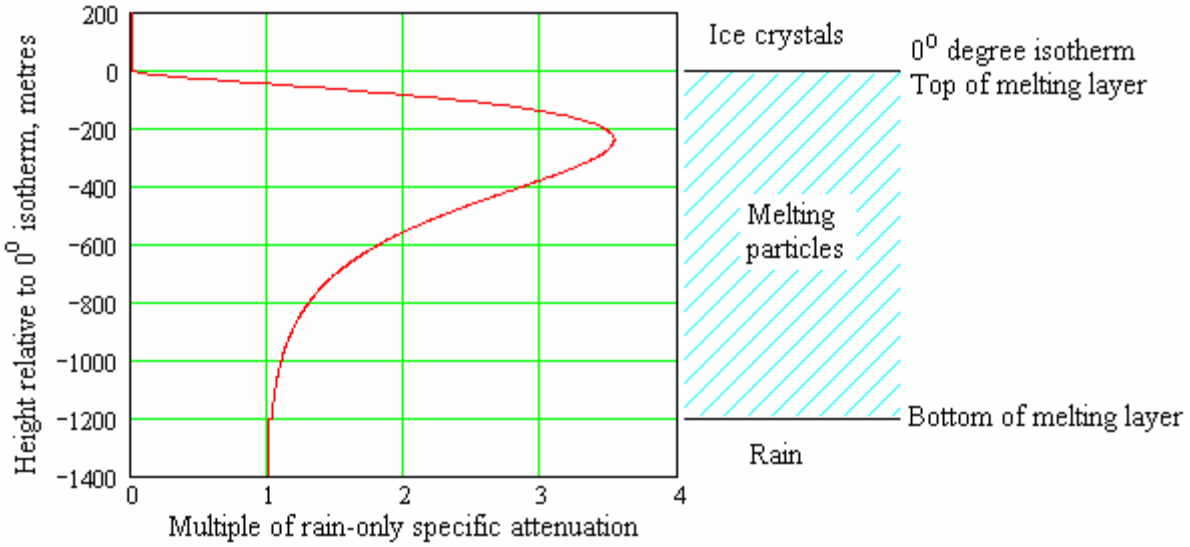

Figure 19 – Gamma factor giving variation of specific attenuation in the melting layer (From 3M45 Annex 9)

To allow for this effect, a correction to the attenuation calculated for rain only is made in the form of a multiplicative factor:

$$A_{rs} = A_p \cdot F \tag{18}$$

The value of the correction factor defaults to unity for regions where this additional loss does not occur. As this model was only recently developed and was extensively tested against data, it is proposed that this method be retained for the WRPM.

UK Rain Statistics

Figure 6 presented some rain rate statistics for the UK. These have been obtained by analysis of Midas data from the BADC. The location of the rapid response rain gagues is shown in Figure 20. As this data is owned by the UK Met office, the data can not be used commercially but it can be used for determining if a model is appropriate. Specifically, permission has been granted to analyse the data to provide distributions for the ITU-R databanks.

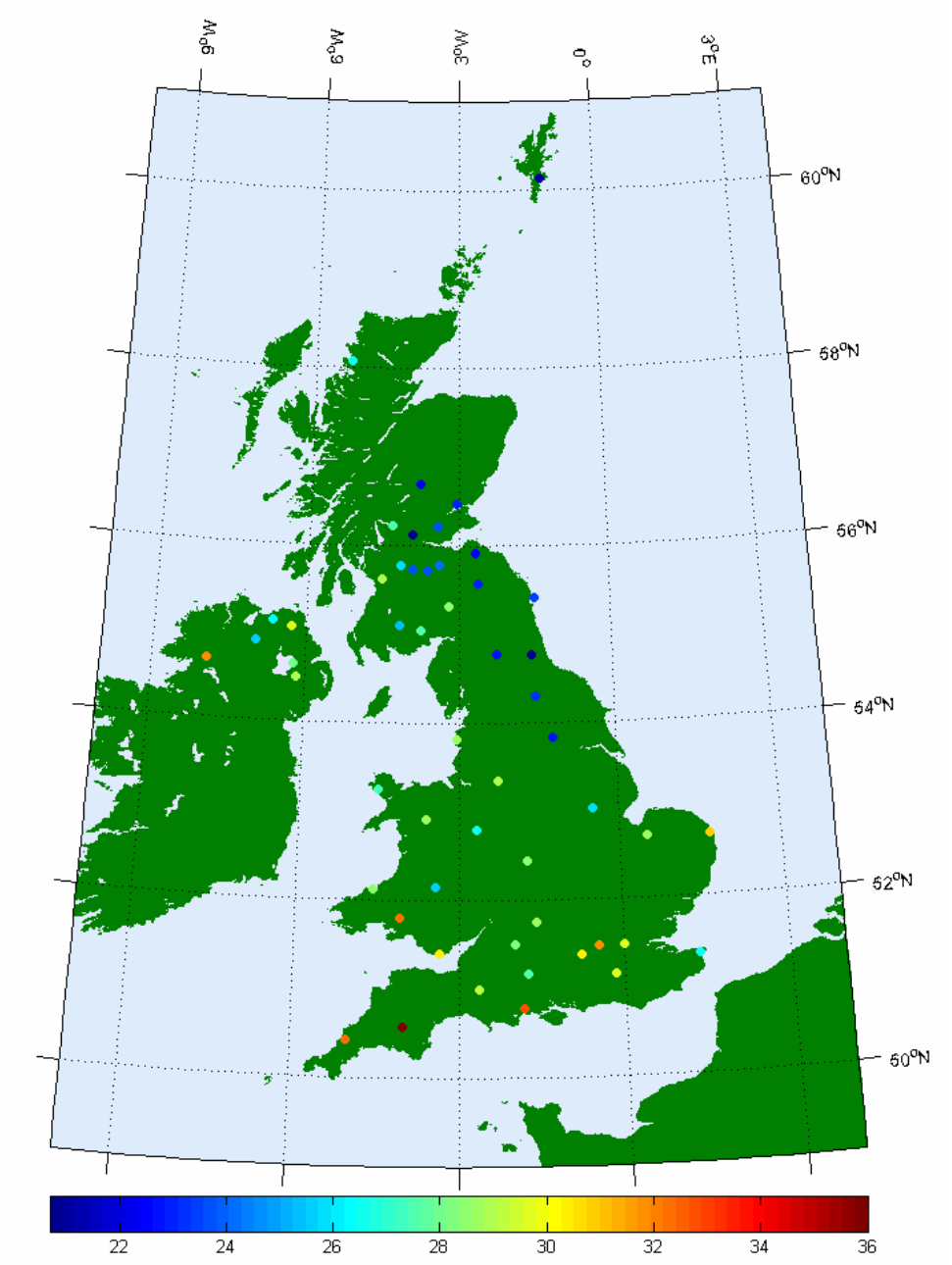

Figure 20 – UK Rapid response rain gauge locations and associated 0.01% rain rates

An example of some data is given in Figure 21 for three years from the 1987-2005 data base. This site was chosen as it has a typical UK climate and was operational for much of the time period. This

demonstrates that the rain rate is variable between years, especially for small time percentages. Higher time percentages appear to be much more stable.

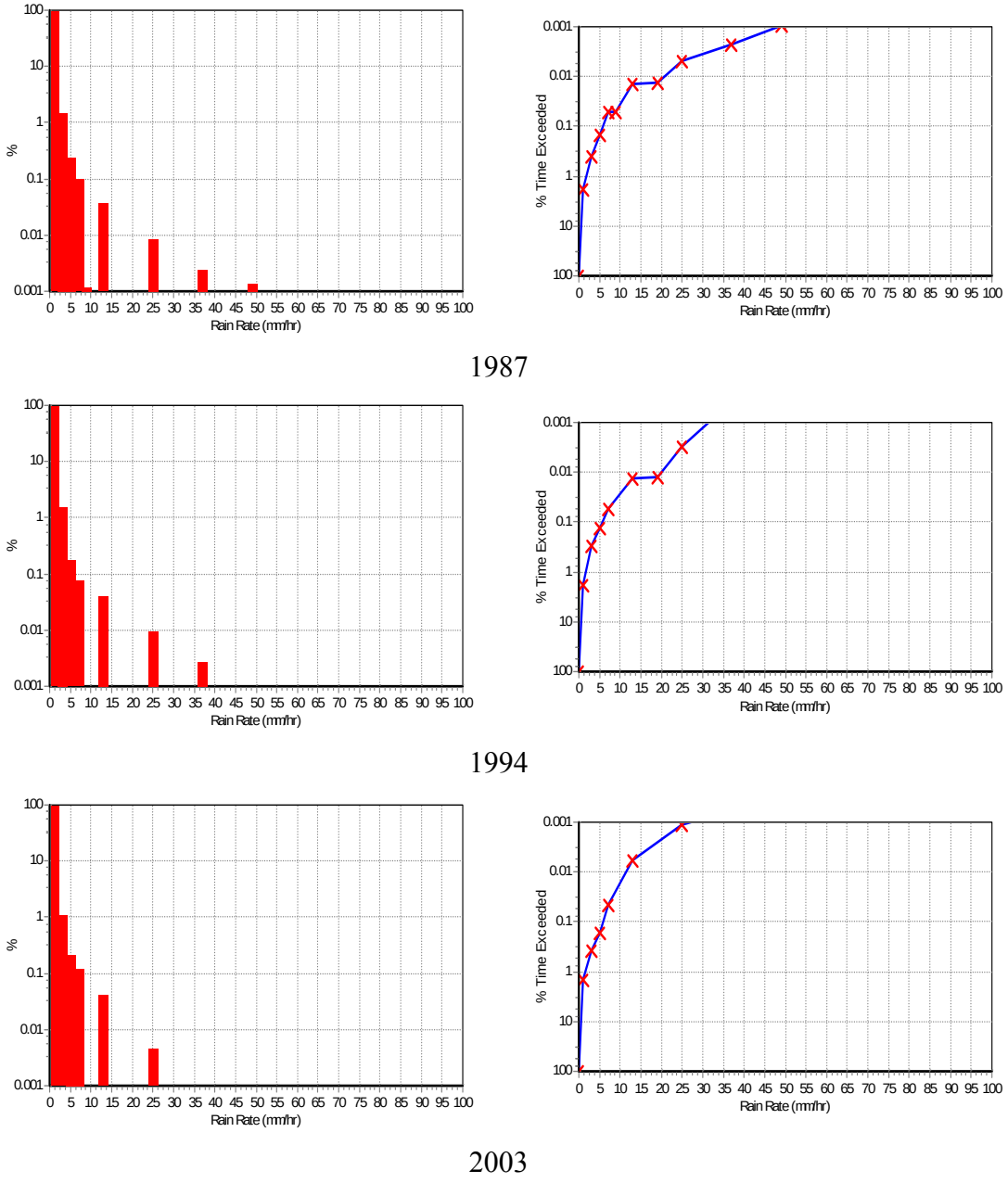

Figure 21 – Some sample rain rate data from Brize Norton

Figure 21 also demonstrates a difficulty with this type of data, there is quantisation evident which is due to the tipping bucket rain gauge. At higher rates the bucket can only tip an integral number of times per minute. As each tip represents 0.2mm of rain, we end up with 12mm/hr quantisation[5] because we can only record 12, 24, 36 and 48 mm/hr rain rates. As this analysis was into 2mm wide sample bins, we only see the 12-14, 24-26, 36-38 and 48-50 mm/h bins populated, which leads to unsmooth CDFs even for long sample periods as demonstrated by Figure 22. Drop counting rain gauges overcome this limitation to a large extent, but we have only limited data of this type. Figure

[5] 12mm/hr = 0.2mm per tip x 60 minutes per hour

22 shows the 0.01% rain rate for Brize Norton based on all 16.7 years of data to be ~22 mm/hr which is as expected.

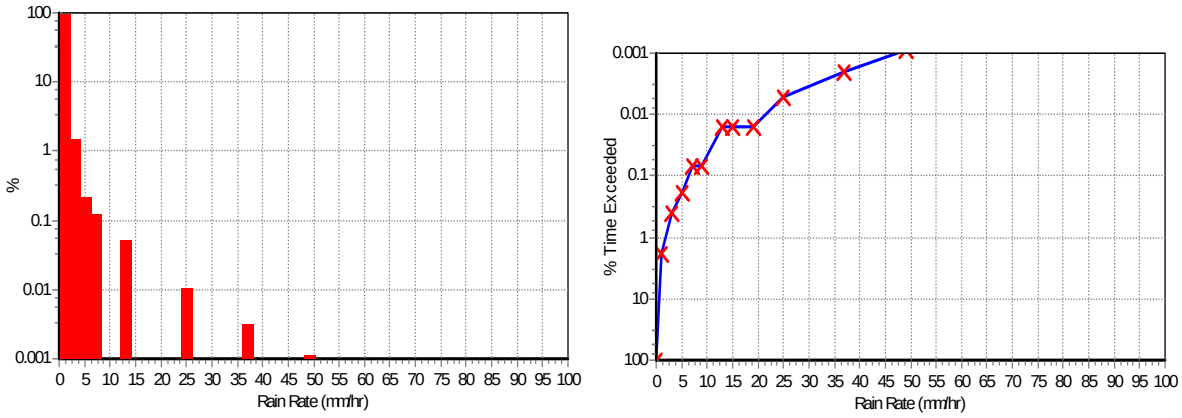

Figure 22 – Brize Norton 1987-2005 rain rate data

Maximum possible rain rate.

It is necessary to define a maximum rain rate for a 0-100% model. Figure 23 shows the recorded rain rates rarely exceed 100mm/hr for any site, but the maximum rain rate that may occur is unknown and it is probable that the rain monitoring equipment may saturate.

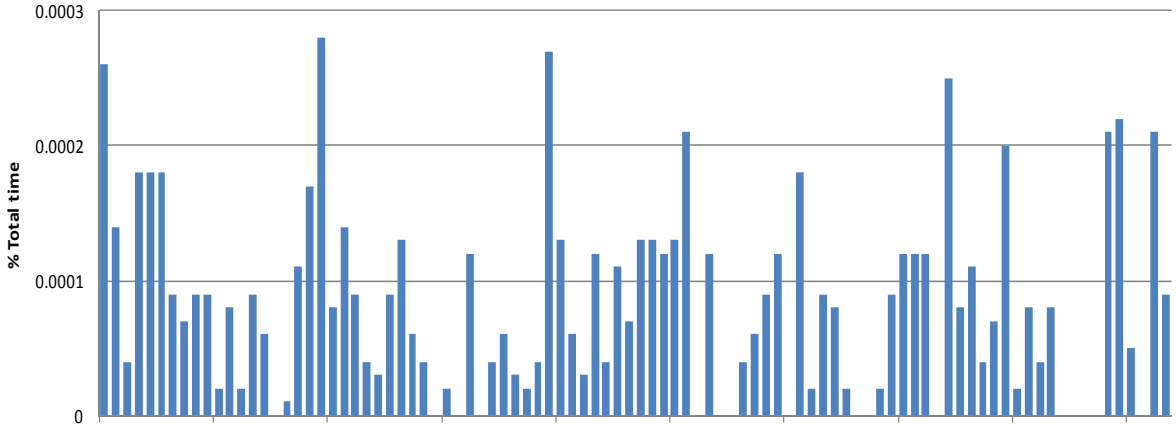

Figure 23 – Percentage time rain rate exceeds 100mm/hr

Figure 24 shows the averaged statistics for the complete data set, concentrating on the higher rain rates. The solid green line represents the average and the markers the maximum and minimum. The statistics become noisy towards the tail of the distribution as we would expect. A rather speculative trend line has been fitted to the average rate which indicates we might expect a one minute averaged rain rate in excess of 300mm/hr once every 20 years.

Given this, the maximum rates recorded in the database are quite surprising. For example Blackpool indicates a rate of around 450mm/hr at 0.0001% (30 seconds per year). Our suspicions are that these exceptional rates are measurement errors, for example from the sudden clearing of a blocked gauge.

The result appears smooth and this site has 16 years of data, so this rate must have occurred 8 times. We can not easily ignore this result and the data up to around 300mm/h looks quite reasonable.

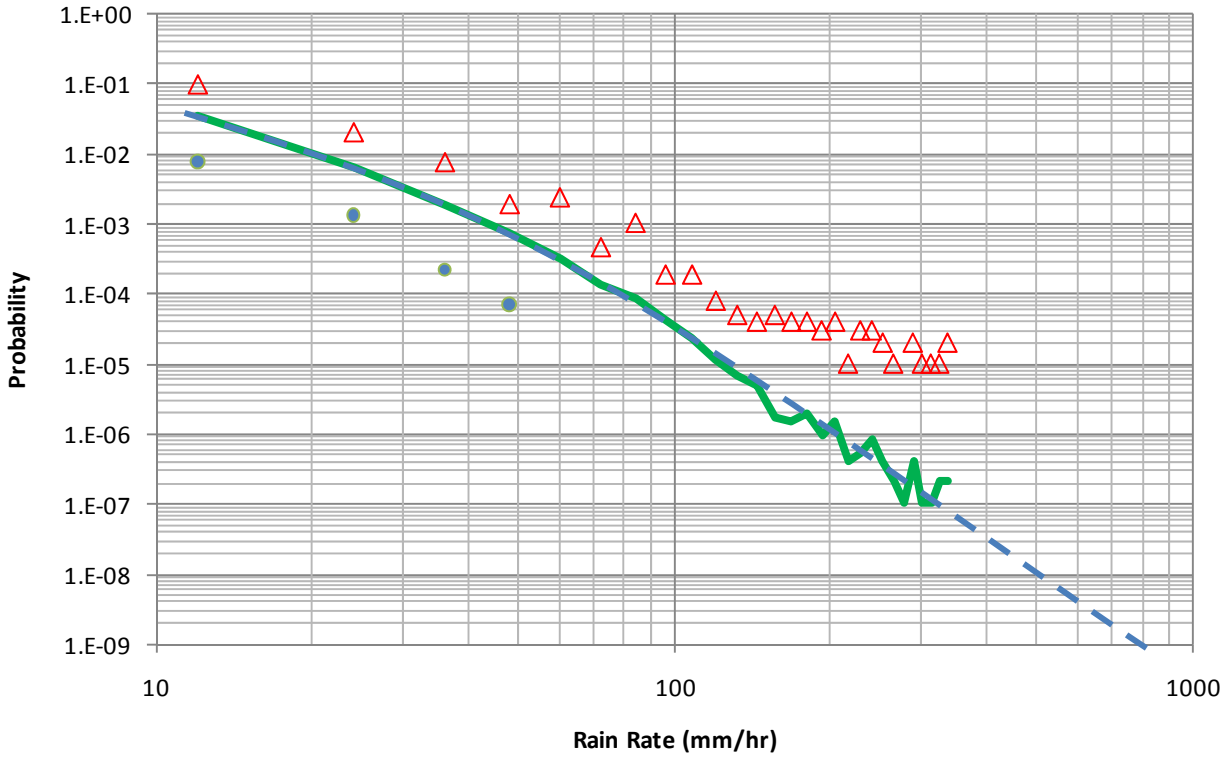

Figure 24 – Rain rate max, min and average for complete data set

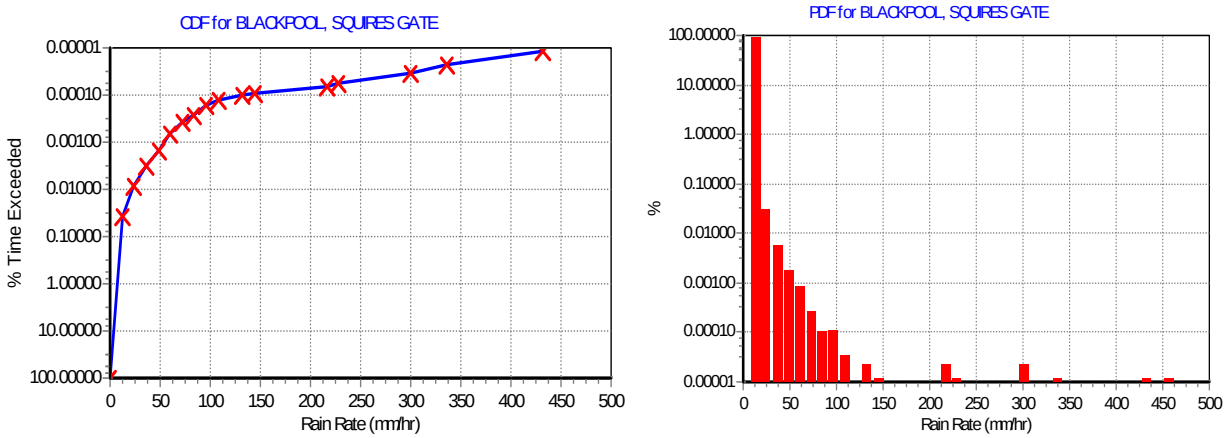

Figure 25 – Highest rain rates recorded

The highest measurement was recorded for Builth Wells, with the result of over 500mm/hr. It is believed this must be an equipment fault. For the WRPM a safe limit could be set at 500 mm/hr.

Rain Time

Recommendation P.837-5 provides a value for the rain time, this has been plotted for the SSER sites in Figure 26. The average value is 5.8%. Recent work has shown a large disparity between the figures given in ITU-R P.836-5 and UK measurement data for the 0.01% rain rate. We may question the accuracy of the rain probability predictions and so make a comparison with data derived from measurements.

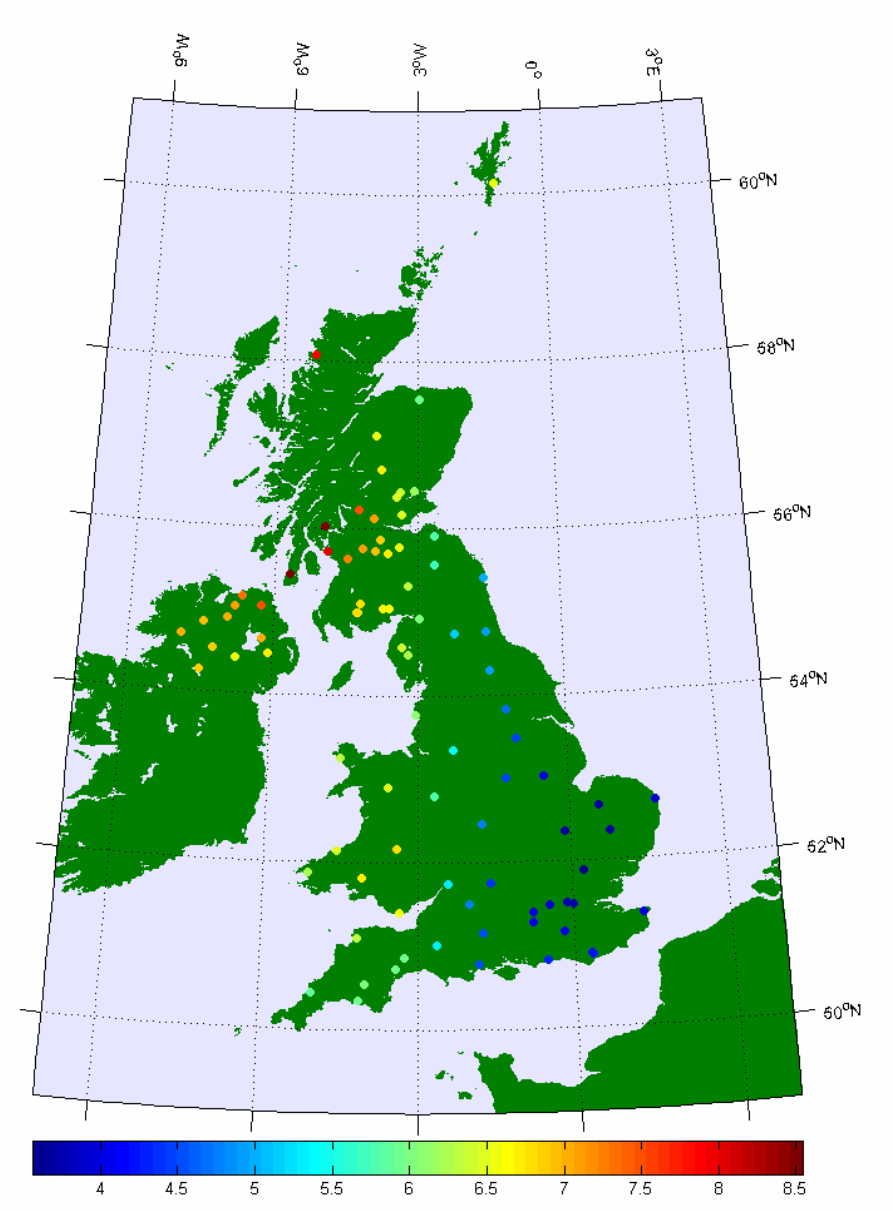

Figure 26 – Rain probability from ITU-R P837-5

It is not easy to tell if it is raining or not based on the SSER data. This is because the measurement is based on the time it takes to collect a fixed volume of rain, resulting in a time lag between the commencement of rain and any measurement. The volume may have accumulated over a long or a short period. We can not compensate for this as rain does not generally start, fall at a constant rate

and then stop. The method used to move from event based statistics to time series will have an effect on the results, for example if a fixed integration time is applied, the minimum and maximum rain rates will be determined by integration which define the minimum rain rate and also average out peaks. For example a during light rain, a 10 minute integration can contain a minimum of 1 0.2mm tip and this is equivalent to 1.2mm/hr which for this application is probably not too serious. However, for rain fading we are interested in peak rain rates at one minute integration. Figure 27 shows a sample of raw recorded data from the Church Fenton gauge. The maximum one minute rain rate recorded is 1.6mm per minute which is 96mm/hr.

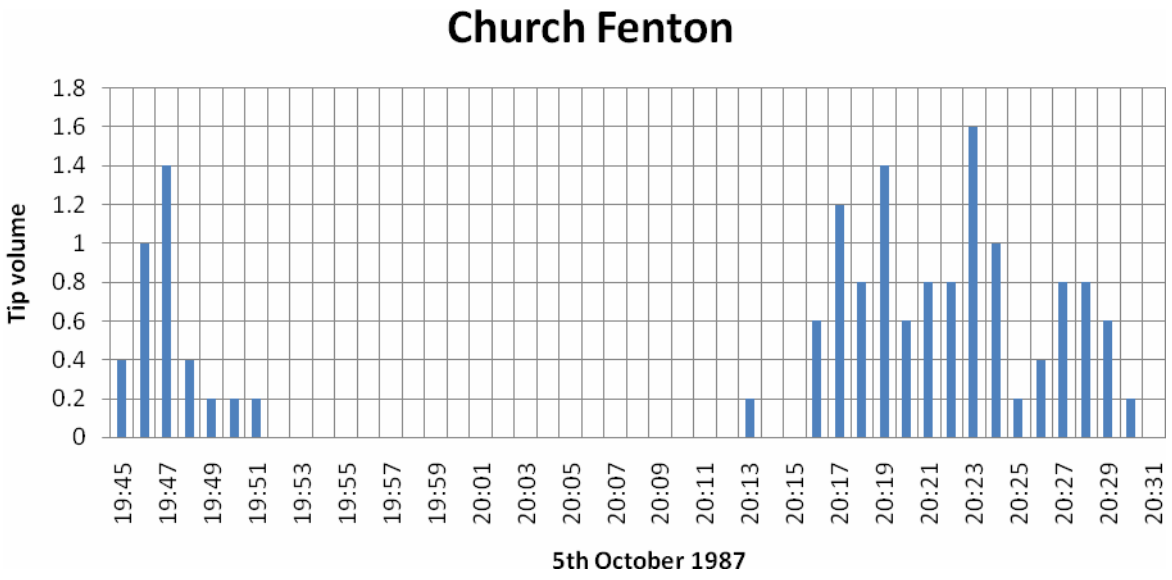

Figure 27 – Example of recorded rain

Figure 28 shows the effect of integrating over a fixed period and demonstrates that this is not a useful approach. Peaks are underestimated and the raining time is exaggerated.

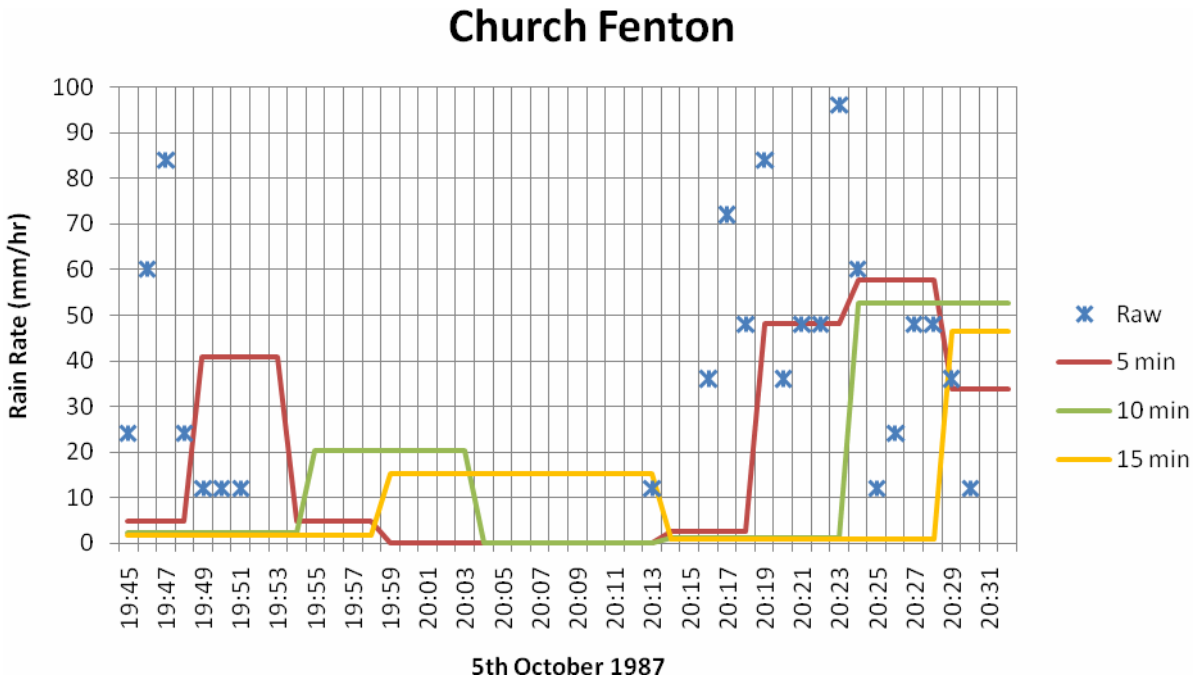

Figure 28 – Effect of integration time

The method used in developing the rain statistics was to integrate the recorded volume over the period since the last recorded tip. This is making the reasonable assumption that the tipping bucket is filling up over the entire period, but also the unreasonable assumption it is filling at a uniform rate. Figure 29 shows the results of this.

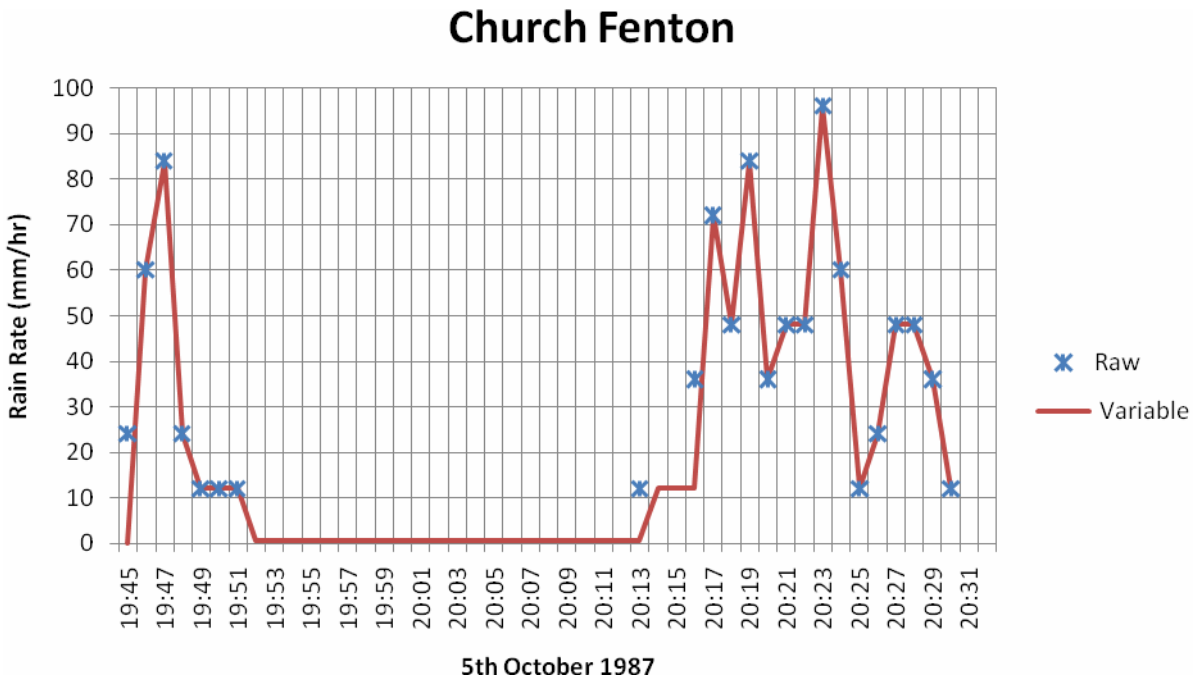

Figure 29 – Integrating over period since last tip

While this approach has a serious weakness in the variable integration time and a secondary problem in that it will appear that it is always raining, it is believed to be a reasonable compromise. We may be able to overcome the continuous rain problem with a threshold and the method does properly record peak rain rates.

In this method, it may be worthwhile limiting the maximum period for rain accumulation; Rain gauges are not very good at measuring low rain rates, some of the rain collected in the instrument will evaporate before it can be measured. A maximum limit has not been implemented as it has no effect at all on the higher rain rates and because we have no evidence on which to base the limit. If it is governed by evaporation, we would need to take account of temperature and humidity, data that we do not have available.

We should not be overly concerned about this as the measurement itself has other weaknesses; gauges occasionally become blocked and so fail to record rain. In cold climates, water can freeze in the gauge and rain will only be recorded when the water melts.

To investigate these limitations, a fine resolution study was made of rain rates below 1mm/hr. Figure 30 shows a few examples.

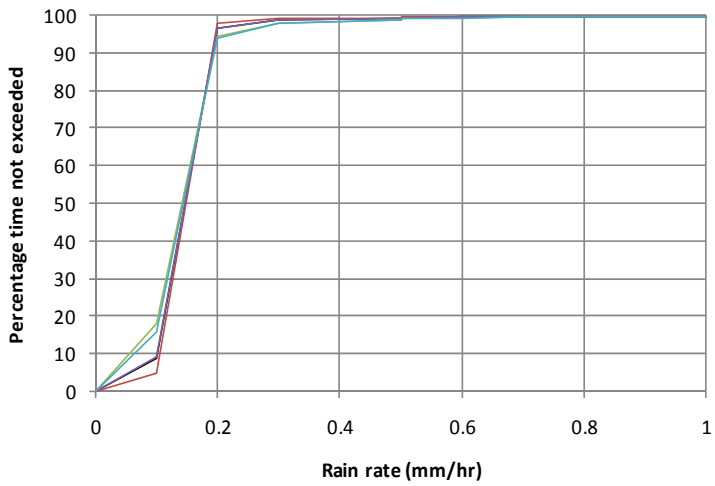

Figure 30 – Percentage time against rain rate

Based on Figure 30, the large step indicates an appropriate threshold appears to be in the range 0.1-0.2mm/hr. This correlated with one tip per hour. Analysis of the complete database showed that for 0.2mm/hr threshold the average total rain time was 7.9%. This figure varied between a minimum of 3% and a maximum of 17% and is clearly quite different from those rates predicted by ITU-R model, which is based on a 0.5mm/hr threshold, where the average was 5.8% and the spread from 3.5% to 8.5%. The reason for this may be the limitations of the SSER gauges, or issues with the ITU-R model. The results for a few different thresholds are shown in Figure 31 through to Figure 33.

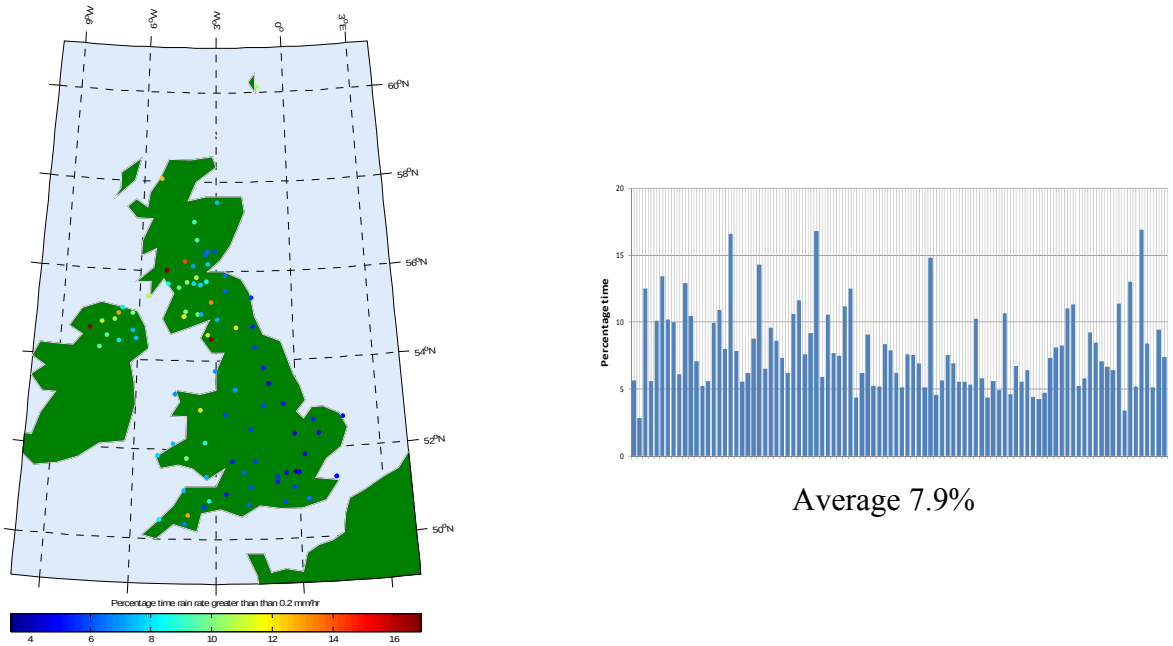

Figure 31 – Percentage time rain rate is above a 0.2mm/hr threshold

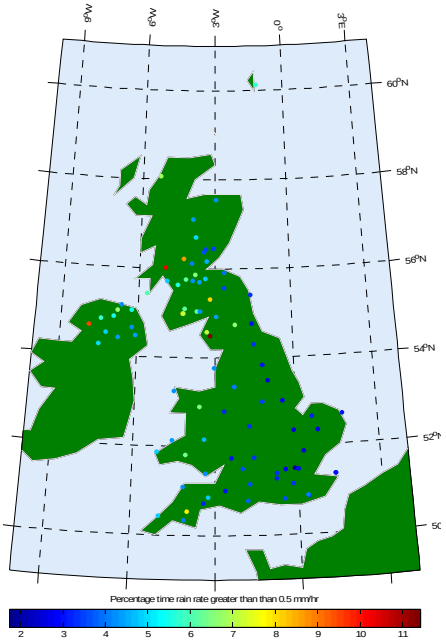

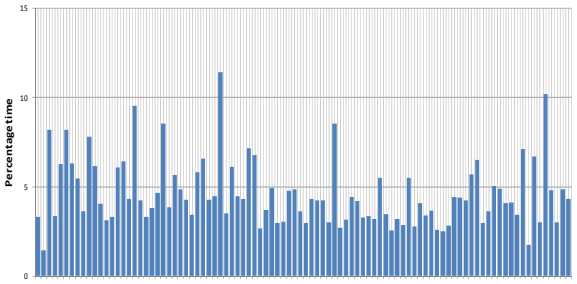

Average 4.6%

Figure 32 – Percentage time rain rate is above a 0.5 mm/hr threshold

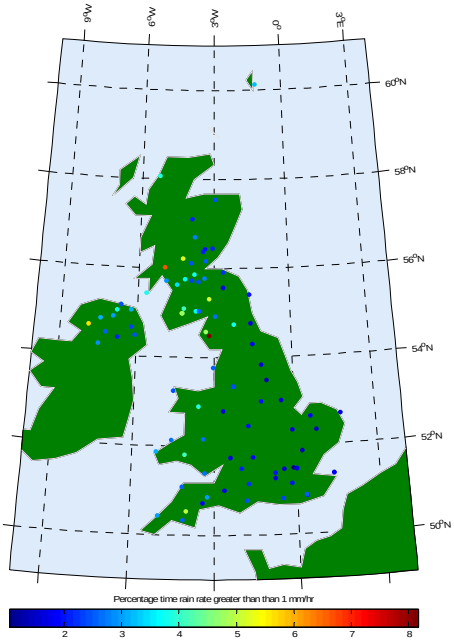

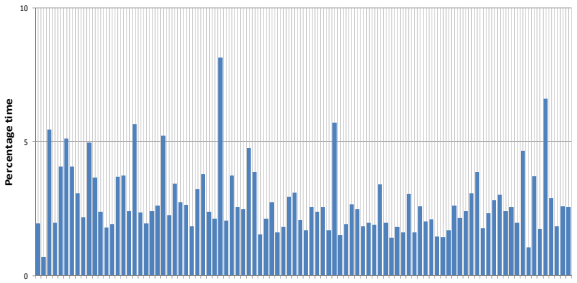

Average 2.7%

Figure 33 – Percentage time rain rate is above a 1mm/hr threshold

The above results demonstrate the problem in obtaining good results based on rain gauge data. They can not give the probability of rain at a site but they do at least give a reasonable bound. The pattern does not change very much though the scales do. The rain time is likely to be strongly affected by local geographic features, so the larger variability in the SSER gauge results is to be expected, however if we can assume the means are representative, the ITU-R model does appear to underestimate the probability of rain. Fortunately, from the viewpoint of the WRPM this error will make little practical difference as the attenuation at these very low rain rates will be small in most applications.

Monthly variability of Heavy Rain

We need to be able to consider worst month as well as annual statistics. In order to test the monthly variability of heavy rain an analysis was made of the number of minutes in each month where the SSER gauges recorded two or more tips per minute. As each tip requires 0.2mm of rain this represents a rain rate of 24mm/hr which is roughly equivalent to that not exceeded for more than

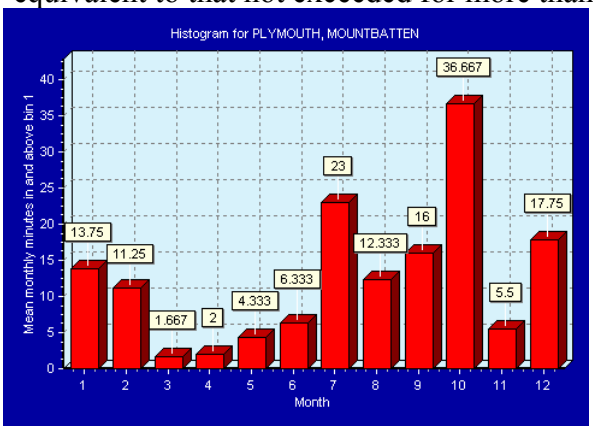

0.01% of the year. Some examples are shown in Figure 34.

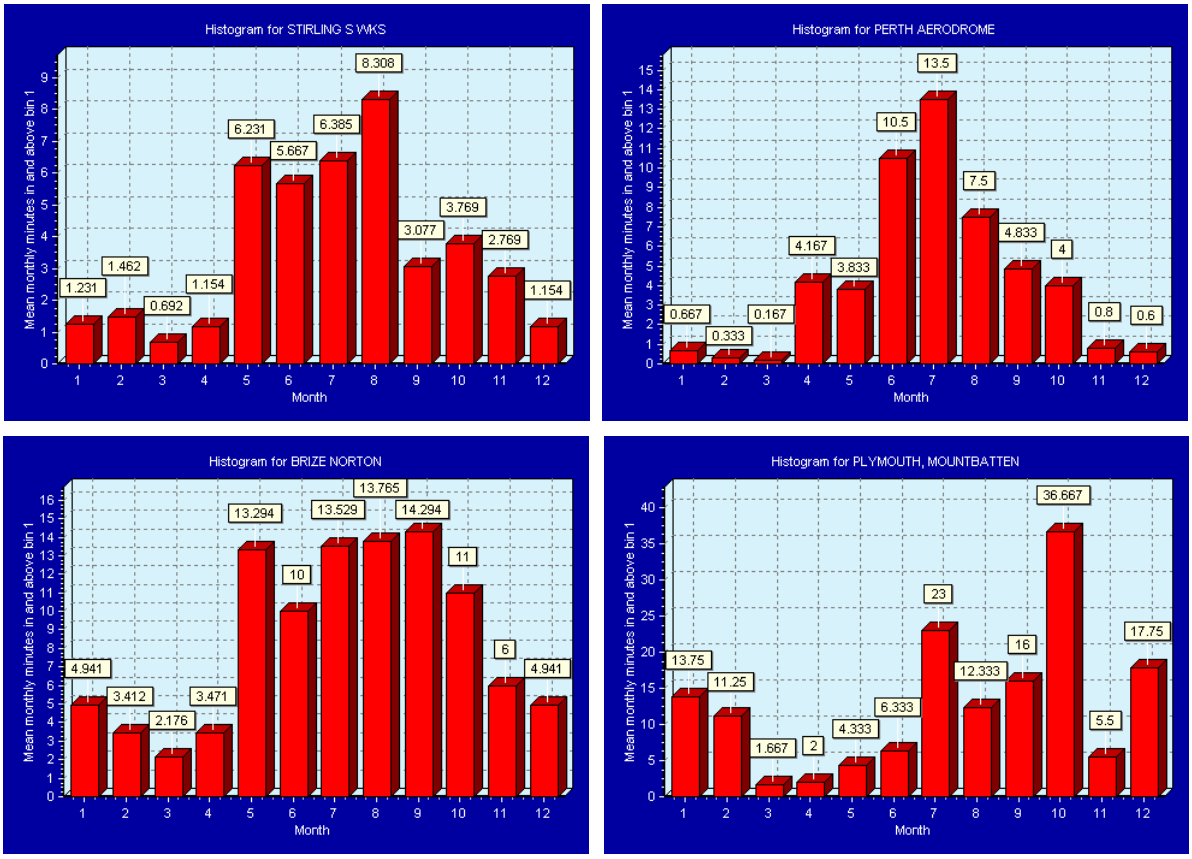

Figure 34 – Examples of the number of minutes per month where rain rate exceeded 24mm/hr

The monthly occurrence of heavy rain was found to vary between sites with a peak generally in the summer months. The average result for the complete dataset is shown in Figure 35.

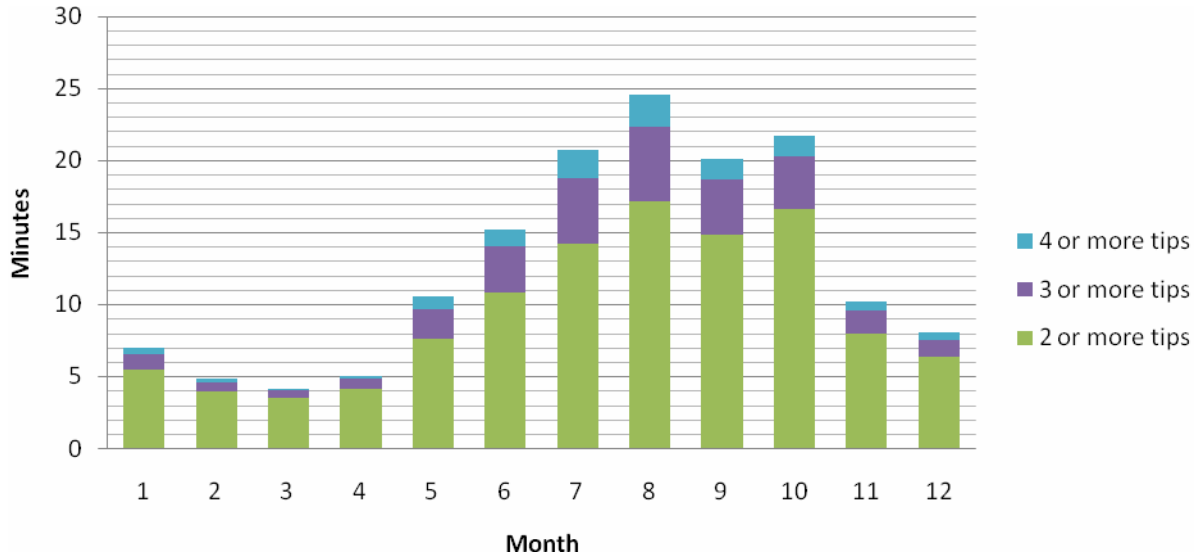

Figure 35 – Database average minutes per month with more than one tip

For two or more tips, the difference between the best and worst month is a factor of five. The peak to mean ratio is demonstrated by Figure 36. Here the monthly minutes are compared with the annual mean showing roughly a factor of 2.4 in time between annual and the worth month, i.e. if a link is designed to suffer rain outage for no more than 0.01% annually, it will suffer 0.024% outage in the worst month.

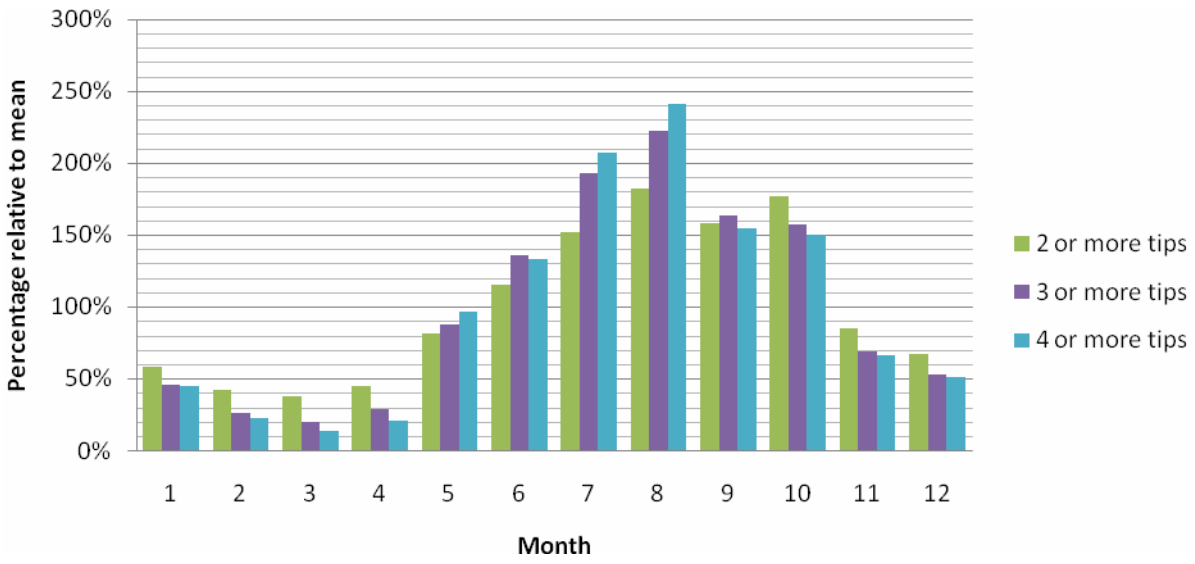

Figure 36 – Monthly variability of higher rain rates compared to annual mean

While heavier rain appears more likely in the summer this does not imply that the amount of rain is higher in the summer. Figure 37 shows the total accumulation of rain per month which is predominantly recorded in single tip minutes, which represent light rain at a rate of less than 12mm/hr.

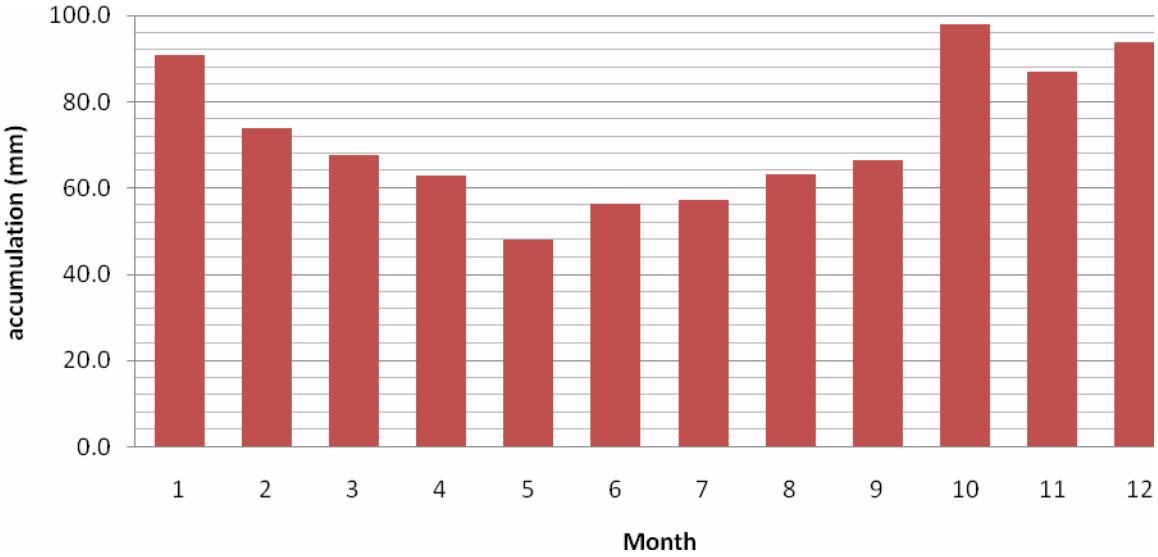

Figure 37 – Rain accumulation

ITU-R format Rain Rate Statistics

It is hoped to be able to process some of the data into the ITU-R format for submission at the next meeting. Unfortunately an NERC bid to fund the full processing of the data was unsuccessful and therefore the processing has been limited to the rain intensity in the format shown in Figure 38.

Part IV: Radiometeorological data

TABLE IV-1 – *Statistics of rain intensity*

Station number _____

RG site name _____

RG country(1) __

RG latitude (–90..+90) (degrees) ___.____

RG longitude (0..360) (degrees) E ___.____

RG altitude amsl h_g (m) ____

Rain zone(2) _

Measurement: Experiment No. ___

Rain gauge type _____

RG resolution (mm/h) ____.___

RG integration time (s) ____

RG accumulation per tip (mm/tip) _.____

RG aperture (cm^2) ____._

Start date (yyyy.mm.dd) ____.__.__

End date (yyyy.mm.dd) ____.__.__

Duration d (days) _____.___

Percentage of year where $R > 0.5$ mm/h p_0 (%) _.__

Table a:

Rain rate exceeded for percentage of year R_a (mm/h)
Rain rate exceeded for percentage of worst month R_{wm} (mm/h)

Percentage of time	0.001 0.1	0.002 0.2	0.003 0.3	0.005 0.5	0.01 1	0.02 2	0.03 3	0.05 5
Rain rate of year R_a (mm/h)	– –	– –	– –	– –	– –	– –	– –	– –
Rain rate of worst month R_{wm} (mm/h)	– –	– –	– –	– –	– –	– –	– –	– –

Table b(3):

Monthly variation of rain
Rain rate exceeded for 0.01%, 0.1% and 1% of the month
Total accumulation of rain during one month

Month of year	Jan	Feb	Mar	Apr	May	Jun	Jul	Aug	Sep	Oct	Nov	Dec
R 0.01 (mm/h)												
R 0.1 (mm/h)												
R 1 (mm/h)												
Total rain (mm)												
Snow included(4)												
RG up-time(5) (%)												

References:

Comments:

(1) See Annex 1 for list of country codes.

(2) See Recommendation ITU-R P.837.

(3) Wherever possible, cumulative distributions for individual years (= 12 consecutive months) are preferred. For multi-year data, one form per year should be used. However, where long term climatic data have been analysed and it is impractical to submit individual yearly distributions, multi-year averages should be submitted with detailed description of the data and analysis parameters.

(4) In geographic locations where precipitation in the form of ice or snow may occur, an explanation should be given as to when and how long these conditions prevail and how the rain gauge data is treated during these intervals. For Table b, the occurrence of snow is to be indicated as follows: 0: No snow, 1: Snow eliminated from statistics, 2: Equivalent water content of snow was included in the measurements, 3: Other (explain under Comments).

(5) If outages occurred in the measurement of rain, explain under Comments whether rainfall occurred during the outage or not.

Figure 38 – ITU-R Table for statistics of rain intensity

Annex 1 – The P.530-12 Rain Model

2.4 Attenuation due to hydrometeors

Attenuation can also occur as a result of absorption and scattering by such hydrometeors as rain, snow, hail and fog. Although rain attenuation can be ignored at frequencies below about 5 GHz, it must be included in design calculations at higher frequencies, where its importance increases rapidly. A technique for estimating long-term statistics of rain attenuation is given in § 2.4.1. On paths at high latitudes or high altitude paths at lower latitudes, wet snow can cause significant attenuation over an even larger range of frequencies. More detailed information on attenuation due to hydrometeors other than rain is given in Recommendation ITU-R P.840.

At frequencies where both rain attenuation and multipath fading must be taken into account, the exceedance percentages for a given fade depth corresponding to each of these mechanisms can be added.

2.4.1 Long-term statistics of rain attenuation

The following simple technique may be used for estimating the long-term statistics of rain attenuation:

Step 1: Obtain the rain rate $R_{0.01}$ exceeded for 0.01% of the time (with an integration time of 1 min). If this information is not available from local sources of long-term measurements, an estimate can be obtained from the information given in Recommendation ITU-R P.837.

Step 2: Compute the specific attenuation, γ_R (dB/km) for the frequency, polarization and rain rate of interest using Recommendation ITU-R P.838.

Step 3: Compute the effective path length, d_{eff}, of the link by multiplying the actual path length d by a distance factor r. An estimate of this factor is given by:

$$r = \frac{1}{1 + d / d_0} \tag{32}$$

where, for $R_{0.01} \leq 100$ mm/h:

$$d_0 = 35\ \mathrm{e}^{-0.015\, R_{0.01}} \tag{33}$$

For $R_{0.01} > 100$ mm/h, use the value 100 mm/h in place of $R_{0.01}$.

Step 4: An estimate of the path attenuation exceeded for 0.01% of the time is given by:

$$A_{0.01} = \gamma_R\, d_{eff} = \gamma_R\, dr \qquad \text{dB} \tag{34}$$

Step 5: For radio links located in latitudes equal to or greater than 30° (North or South), the attenuation exceeded for other percentages of time p in the range 0.001% to 1% may be deduced from the following power law:

$$\frac{A_p}{A_{0.01}} = 0.12\ p^{-(0.546 + 0.043 \log_{10} p)} \tag{35}$$

This formula has been determined to give factors of 0.12, 0.39, 1 and 2.14 for 1%, 0.1%, 0.01% and 0.001% respectively, and must be used only within this range.

Step 6: For radio links located at latitudes below 30° (North or South), the attenuation exceeded for other percentages of time p in the range 0.001% to 1% may be deduced from the following power law:

$$\frac{A_p}{A_{0.01}} = 0.07\ p^{-(0.855 + 0.139 \log_{10} p)} \tag{36}$$

This formula has been determined to give factors of 0.07, 0.36, 1 and 1.44 for 1%, 0.1%, 0.01% and 0.001%, respectively, and must be used only within this range.

Step 7: If worst-month statistics are desired, calculate the annual time percentages p corresponding to the worst-month time percentages p_w using climate information specified in Recommendation ITU-R P.841. The values of A exceeded for percentages of the time p on an annual basis will be exceeded for the corresponding percentages of time p_w on a worst-month basis.

The prediction procedure outlined above is considered to be valid in all parts of the world at least for frequencies up to 40 GHz and path lengths up to 60 km.

2.4.2 Combined method for rain and wet snow

The attenuation, A_p, exceeded for time percentage p given by the previous sub-section is valid for link paths through which only liquid rain falls.

For high latitudes or high link altitudes, higher values of attenuation may be exceeded for time percentage p due to the effect of melting ice particles or wet snow in the melting layer. The incidence of this effect is determined by the height of the link in relation to the rain height, which varies with geographic location. The variation of zero-degree rain height is taken into account in the following method by taking 49 height values relative to the median of the rain height, with a probability associated with each given by Table 1.

The following method is not needed if it is known that a link is never affected by the melting layer. If this is not known, the calculation for rain given above should be used to calculate A_p, and then the following steps should be followed:

Step 1: Obtain the median rain height, h_{rainm}, metres above mean sea level (amsl) from Recommendation ITU-R P.839.

Step 2: Calculate the rain height of the centre of the link path, h_{link}, taking median-Earth curvature into account using:

$$h_{link} = 0.5(h_1 + h_2) - (D^2/17) \qquad \text{m amsl} \tag{37}$$

where:

$h_{1,2}$: height of the link terminals (amsl)

D: path length (km).

Step 3: A test may now be made to determine whether there is a possibility of additional attenuation. If $h_{link} \leq h_{rainm} - 3\ 600$, the link will not be affected by melting-layer conditions and A_p can be taken as the attenuation exceeded for p% of the time, and this method can be stopped. Otherwise, the method continues with the following steps.

Step 4: Initialize a multiplying factor, F, to zero.

Step 5: For successive values of the index i = 0, 1, 2, to 48, in order:

a) Calculate the rain height, h_{rain}, using:

$$h_{rain} = h_{rainm} - 2400 + 100i \quad \text{m amsl} \tag{38}$$

b) Calculate the link height relative to the rain height using:

$$\Delta h = h_{link} - h_{rain} \quad \text{m} \tag{39}$$

c) Calculate the addition to the multiplying factor for this value of the index i:

$$\Delta F = \Gamma(\Delta h) P_i \tag{40}$$

where:

$\Gamma(\Delta h)$ is a multiplying factor which takes account of differing specific attenuations according to height relative to the rain height, given by:

$$\Gamma(\Delta h) = \begin{cases} 0 & 0 < \Delta h \\ \dfrac{4\left(1 - e^{\Delta h/70}\right)^2}{\left(1 + \left(1 - e^{-(\Delta h/600)^2}\right)^2 \left(4\left(1 - e^{\Delta h/70}\right)^2 - 1\right)\right)} & -1200 \le \Delta h \le 0 \\ 1 & \Delta h < -1200 \end{cases} \tag{41}$$

and P_i is the probability that the link will be at Δh, taken from Table 1.

d) Add ΔF to the current value of F. This operation may be represented as a procedure by the expression:

$$F = F + \Delta F \quad \text{dB} \tag{42}$$

Step 6: Calculate the combined rain and wet snow attenuation using:

$$A_{rs} = A_p \cdot F \tag{43}$$

Depending on the height of the link relative to the median rain height, A_{rs} can be more than or less than A_p. Near the poles of the Earth it is possible for the link to be always above the rain height, in which case A_{rs} is zero.

TABLE 1

Index "*i*"		**Probability P_i**
Either	**Or**	
0	48	0.000555
1	47	0.000802
2	46	0.001139
3	45	0.001594
4	44	0.002196
5	43	0.002978
6	42	0.003976

Index "*i*"		Probability P_i
Either	**Or**	
7	41	0.005227
8	40	0.006764
9	39	0.008617
10	38	0.010808
11	37	0.013346
12	36	0.016225
13	35	0.019419
14	34	0.022881
15	33	0.026542
16	32	0.030312
17	31	0.034081
18	30	0.037724
19	29	0.041110
20	28	0.044104
21	27	0.046583
22	26	0.048439
23	25	0.049588
24		0.049977

2.4.3 Frequency scaling of long-term statistics of rain attenuation

When reliable long-term attenuation statistics are available at one frequency the following empirical expression may be used to obtain a rough estimate of the attenuation statistics for other frequencies in the range 7 to 50 GHz, for the same hop length and in the same climatic region:

$$A_2 = A_1 \, (\Phi_2 / \Phi_1)^{1 - H(\Phi_1, \Phi_2, A_1)} \tag{44}$$

where:

$$\Phi(f) = \frac{f^2}{1 + 10^{-4} \; f^2} \tag{45}$$

$$H(\Phi_1, \Phi_2, A_1) = 1.12 \times 10^{-3} \, (\Phi_2 / \Phi_1)^{0.5} \, (\Phi_1 \, A_1)^{0.55} \tag{46}$$

Here, A_1 and A_2 are the equiprobable values of the excess rain attenuation at frequencies f_1 and f_2 (GHz), respectively.

2.4.4 Polarization scaling of long-term statistics of rain attenuation

Where long-term attenuation statistics exist at one polarization (either vertical (V) or horizontal (H)) on a given link, the attenuation for the other polarization over the same link may be estimated through the following simple formulae:

$$A_V = \frac{300 \, A_H}{335 + A_H} \qquad \text{dB} \tag{47}$$

or

$$A_H = \frac{335\ A_V}{300 - A_V} \qquad \text{dB} \tag{48}$$

These expressions are considered to be valid in the range of path length and frequency for the prediction method of § 2.4.1.

2.4.5 Statistics of event duration and number of events

Although there is little information as yet on the overall distribution of fade duration, there are some data and an empirical model for specific statistics such as mean duration of a fade event and the number of such events. An observed difference between the average and median values of duration indicates, however, a skewness of the overall distribution of duration. Also, there is strong evidence that the duration of fading events in rain conditions is much longer than those during multipath conditions.

An attenuation event is here defined to be the exceedance of attenuation A for a certain period of time (e.g., 10 s or longer). The relationship between the number of attenuation events $N(A)$, the mean duration $D_m(A)$ of such events, and the total time $T(A)$ for which attenuation A is exceeded longer than a certain duration, is given by:

$$N(A) = T(A) / D_m(A) \tag{49}$$

The total time $T(A)$ depends on the definition of the event. The event usually of interest for application is one of attenuation A lasting for 10 s or longer. However, events of shorter duration (e.g., a sampling interval of 1 s used in an experiment) are also of interest for determining the percentage of the overall outage time attributed to unavailability (i.e., the total event time lasting 10 s or longer).

The number of fade events exceeding attenuation A for 10 s or longer can be represented by:

$$N_{10\,s}(A) = a\,A^b \tag{50}$$

where a and b are coefficients that are expected to depend on frequency, path length, and other variables such as climate.

On the basis of one set of measurements for an 18 GHz, 15 km path on the Scandinavian peninsula, values of a and b estimated for a one-year period are:

$$a = 5.7 \times 10^5 \qquad b = -3.4 \tag{51}$$

Once $N_{10\,s}(A)$ has been obtained from equation (50), the mean duration of fading events lasting 10 s or longer can be calculated by inverting equation (49).

Based on the noted set of measurements (from an 18 GHz, 15 km path on the Scandinavian peninsula), 95-100% of all rain events greater than about 15 dB can be attributed to unavailability. With such a fraction known, the availability can be obtained by multiplying this fraction by the total percentage of time that a given attenuation A is exceeded as obtained from the method of § 2.4.1.

2.4.6 Rain attenuation in multiple hop networks

There are several configurations of multiple hops of interest in point-to-point networks in which the non-uniform structure of hydrometeors plays a role. These include a series of hops in a tandem network and more than one such series of hops in a route-diversity network.

2.4.6.1 Length of individual hops in a tandem network

The overall transmission performance of a tandem network is largely influenced by the propagation characteristics of the individual hops. It is sometimes possible to achieve the same overall physical connection by different combinations of hop lengths. Increasing the length of individual hops inevitably results in an increase in the probability of outage for those hops. On the other hand, such a move could mean that fewer hops might be required and the overall performance of the tandem network might not be impaired.

2.4.6.2 Correlated fading on tandem hops

If the occurrence of rainfall were statistically independent of location, then the overall probability of fading for a linear series of links in tandem would be given to a good approximation by:

$$P_T = \sum_{i=1}^{n} P_i \tag{52}$$

where P_i is the probability of fading for the i-th of the total n links.

On the other hand, if precipitation events are correlated over a finite area, then the attenuation on two or more links of a multi-hop relay system will also be correlated, in which case the combined fading probability may be written as:

$$P_T = K \sum_{i=1}^{n} P_i \tag{53}$$

where K is a modification factor that includes the overall effect of rainfall correlation.

Few studies have been conducted with regard to this question. One such study examined the instantaneous correlation of rainfall at locations along an East-West route, roughly parallel to the prevailing direction of storm movement. Another monitored attenuation on a series of short hops oriented North-South, or roughly perpendicular to the prevailing storm track during the season of maximum rainfall.

For the case of links parallel to the direction of storm motion, the effects of correlation for a series of hops each more than 40 km in length, l, were slight. The modification factor, K, in this case exceeded 0.9 for rain induced outage of 0.03% and may reasonably be ignored (see Fig. 5). For shorter hops, however, the effects become more significant: the overall outage probability for 10 links of 20, 10 and 5 km each is approximately 80%, 65% and 40% of the uncorrelated expectation, respectively (modification factors 0.8, 0.65, 0.4). The influence of rainfall correlation is seen to be somewhat greater for the first few hops and then decreases as the overall length of the chain increases.

The modification factors for the case of propagation in a direction perpendicular to the prevailing direction of storm motion are shown in Fig. 6 for several probability levels. In this situation, the modification factors fall more rapidly for the first few hops (indicating a stronger short-range correlation than for propagation parallel to storm motion) and maintain relatively steady values thereafter (indicating a weaker long-range correlation).

2.4.6.3 Route-diversity networks

Making use of the fact that the horizontal structure of precipitation can change significantly within the space of a fraction of a kilometre, route diversity networks can involve two or more hops in

tandem in two or more diversity routes. Although there is no information on diversity improvement for complete route diversity networks, there is some small amount of information on elements of such a network. Such elements include two paths converging at a network node, and approximately parallel paths separated horizontally.

FIGURE 5

Modification factor for joint rain attenuation on a series of tandem hops of equal length, *l*, for an exceedance probability of 0.03% for each link

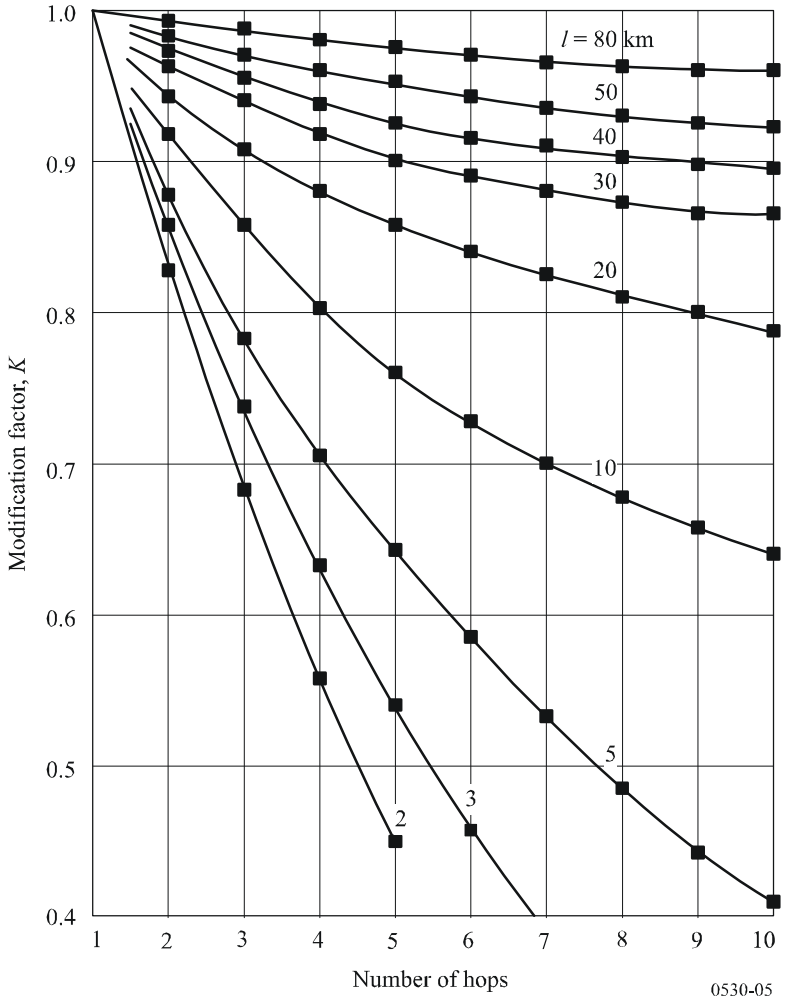

2.4.6.3.1 Convergent path elements

Information on the diversity improvement factor for converging paths in the low EHF range of the spectrum can be found in Recommendation ITU-R P.1410. Although developed for point-to-area applications, it can be used to give some general indication of the improvement afforded by such elements of a point-to-point route-diversity (or mesh) network, of which there would be two.

Due to the random temporal and spatial distribution of the rainfall rate, convergent point-to-point links will instantaneously experience different depths of attenuation. As a result, there may be a degradation in the *S*/*I* between links from users in different angular sectors whenever the desired signal is attenuated by rain in its path and the interfering signal is not.

The differential rain attenuation cumulative distribution for two convergent links operating at the same frequency can be estimated by (see Note 1):

$$A_{12}(p) = \left[A_1(p) - 0.34\, A_2(p)\right] \left(2.65\, |\theta|^{0.23} + 0.004\, |\Delta d|^{2.25}\right) f^{-0.4} \quad \text{dB} \qquad (54)$$

where p is the percentage of time, between 0.01% and 1%, f (GHz) is the frequency, Δd (km) the path length difference and θ (rad) is the angle between the links, from 0° to 180°. $A_1(p)$ and $A_2(p)$ are the values of rain attenuation in the individual links exceeded during p% of the time, calculated using the method given in § 2.4.1.

NOTE 1 – Equation (54) is based on the results of measurements on 36 pairs of convergent links with frequencies in the range from 15 to 38 GHz and path lengths in the range of 1 to 23 km.

2.4.6.3.2 Parallel paths separated horizontally

Experimental data obtained in the United Kingdom in the 20-40 GHz range give an indication of the improvement in link reliability which can be obtained by the use of parallel-path elements of route-diversity networks. The diversity gain (i.e. the difference between the attenuation (dB) exceeded for a specific percentage of time on a single link and that simultaneously on two parallel links):

– tends to decrease as the path length increases from 12 km for a given percentage of time, and for a given lateral path separation,

– is generally greater for a spacing of 8 km than for 4 km, though an increase to 12 km does not provide further improvement,

– is not significantly dependent on frequency in the range 20-40 GHz, for a given geometry, and

– ranges from about 2.8 dB at 0.1% of the time to 4.0 dB at 0.001% of the time, for a spacing of 8 km, and path lengths of about the same value. Values for a 4 km spacing are about 1.8 to 2.0 dB.

FIGURE 6

Modification factor for joint rain attenuation on a series of tandem hops of a approximately 4.6 km each for several exceedance probability levels for each link

(May 1975-March 1979)

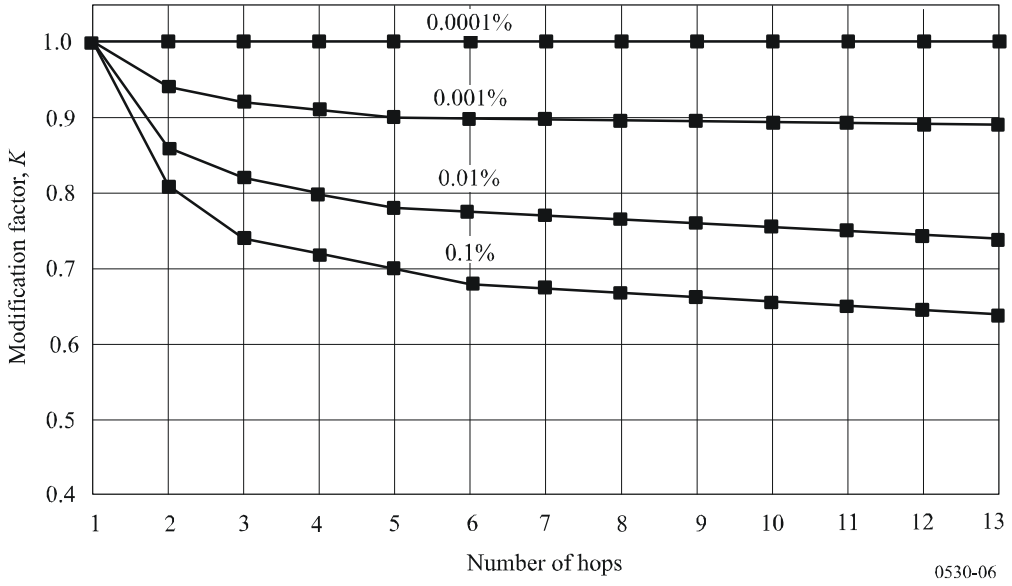

2.4.6.4 Paths with passive repeaters

2.4.6.4.1 Plane-reflector repeaters

For paths with two or more legs (N in total) for which plane passive reflectors are used and for which the legs are within a few degrees of being parallel (see Note 1), calculate the rain attenuation on the overall path by substituting the path length.

$$d = d_{leg1} + d_{leg2} + ... + d_{legN} \quad \text{km} \tag{55}$$

into the method of § 2.4.1, including into the calculation of the distance reduction factor from equation (32).

NOTE 1 – No strict guideline can be given at the present time on how closely the legs should be parallel. If the legs are not parallel, the approach in equation (55) will result in a reduction factor r in equation (32) that is smaller than it should be, thus causing the actual total attenuation to be underestimated. A possible solution to this might be to employ both equation (55) and the path length obtained by joining the ends of first and last leg in the calculation of the reduction factor alone, and averaging the results.

An alternative approach might be to treat the legs as independent paths and apply the information in § 2.4.6.

2.4.6.4.2 Back-to-back-antenna repeaters

If the two or more legs of the path use the same polarization, calculate the attenuation statistics using the method of § 2.4.6.4.1 for plane reflectors.

If the legs of the path use different polarizations, apply the method of § 2.4.1 along with equation (55) for both horizontal and vertical polarization to obtain the percentages of time p_H and p_V for which the desired attenuation is exceeded (see Note 1) with horizontal and vertical polarization, respectively. Use equation (55) to calculate the total path length d_H for those legs using horizontal polarization and also to calculate the total path length d_V for those legs using vertical

polarization. Then calculate the percentage of time p that the given attenuation is exceeded on the overall path from (see Note 2):

$$p = \frac{p_H d_H + p_V d_V}{d_H + d_V} \quad \% \tag{56}$$

NOTE 1 – Since the method of § 2.4.1 provides the attenuation exceeded for a given percentage of time, it must be inverted numerically to obtain the percentage of time that a given attenuation is exceeded.

NOTE 2 – If the legs of the path deviate significantly from being parallel to one another, it is likely that an approach similar to that suggested in Note 1 of § 2.4.6.4.1 might be employed to improve accuracy. In this case, it would have to be employed to calculate the attenuation for each polarization separately.

2.4.7 Prediction of outage due to precipitation

In the design of a digital link, calculate the probability, P_{rain}, of exceeding a rain attenuation equal to the flat fade margin F (dB) (see § 2.3.5) for the specified BER from:

$$P_{rain} = p/100 \tag{57}$$

where p (%) is the percentage of time that a rain attenuation of F (dB) is exceeded in the average year by solving equation (35) in § 2.4.1.

Annex 2 – The P618-9 Rain model

2.2 Attenuation by precipitation and clouds

2.2.1 Prediction of attenuation statistics for an average year

The general method to predict attenuation due to precipitation and clouds along a slant propagation path is presented in § 2.2.1.1.

If reliable long-term statistical attenuation data are available that were measured at an elevation angle and a frequency (or frequencies) different from those for which a prediction is needed, it is often preferable to scale these data to the elevation angle and frequency in question rather than using the general method. The recommended frequency-scaling method is found in § 2.2.1.2.

Site diversity effects may be estimated with the method of § 2.2.4.

2.2.1.1 Calculation of long-term rain attenuation statistics from point rainfall rate

The following procedure provides estimates of the long-term statistics of the slant-path rain attenuation at a given location for frequencies up to 55 GHz. The following parameters are required:

$R_{0.01}$: point rainfall rate for the location for 0.01% of an average year (mm/h)

h_s: height above mean sea level of the earth station (km)

θ: elevation angle (degrees)

φ: latitude of the earth station (degrees)

f: frequency (GHz)

R_e: effective radius of the Earth (8 500 km).

If local data for the earth station height above mean sea level is not available, an estimate can be obtained from the maps of topographic altitude given in Recommendation ITU-R P.1511.

The geometry is illustrated in Fig. 1.

FIGURE 1

Schematic presentation of an Earth-space path giving the parameters to be input into the attenuation prediction process

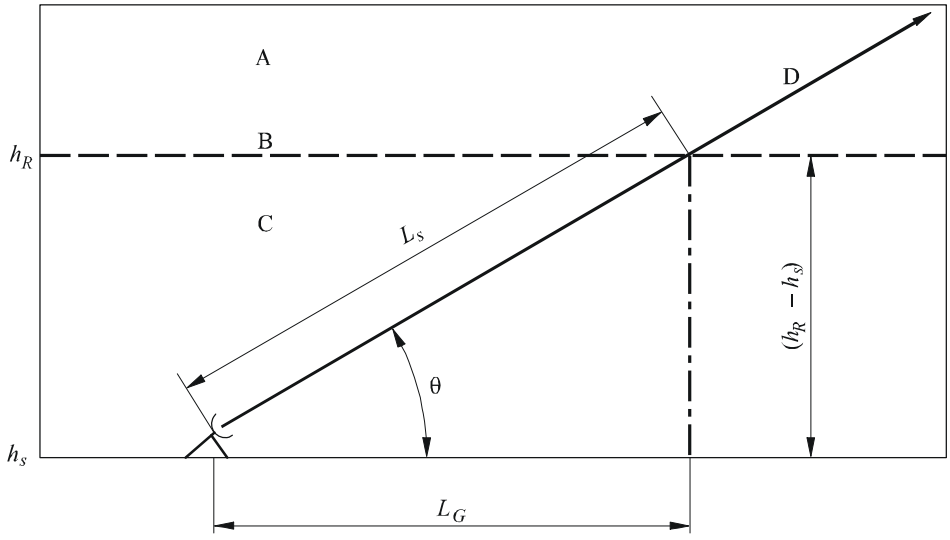

A: frozen precipitation
B: rain height
C: liquid precipitation
D: Earth-space path

0618-01

Step 1: Determine the rain height, h_R, as given in Recommendation ITU-R P.839.

Step 2: For $\theta \geq 5°$ compute the slant-path length, L_s, below the rain height from:

$$L_s = \frac{(h_R - h_s)}{\sin\theta} \quad \text{km} \tag{1}$$

For $\theta < 5°$, the following formula is used:

$$L_s = \frac{2(h_R - h_s)}{\left(\sin^2\theta + \frac{2(h_R - h_s)}{R_e}\right)^{1/2} + \sin\theta} \quad \text{km} \tag{2}$$

If $h_R - h_s$ is less than or equal to zero, the predicted rain attenuation for any time percentage is zero and the following steps are not required.

Step 3: Calculate the horizontal projection, L_G, of the slant-path length from:

$$L_G = L_s \cos\theta \quad \text{km} \tag{3}$$

Step 4: Obtain the rainfall rate, $R_{0.01}$, exceeded for 0.01% of an average year (with an integration time of 1 min). If this long-term statistic cannot be obtained from local data sources, an estimate can be obtained from the maps of rainfall rate given in Recommendation ITU-R P.837. If $R_{0.01}$ is equal to zero, the predicted rain attenuation is zero for any time percentage and the following steps are not required.

Step 5: Obtain the specific attenuation, γ_R, using the frequency-dependent coefficients given in Recommendation ITU-R P.838 and the rainfall rate, $R_{0.01}$, determined from Step 4, by using:

$$\gamma_R = k\,(R_{0.01})^{\alpha} \qquad \text{dB/km} \tag{4}$$

Step 6: Calculate the horizontal reduction factor, $r_{0.01}$, for 0.01% of the time:

$$r_{0.01} = \frac{1}{1 + 0.78\sqrt{\frac{L_G\,\gamma_R}{f}} - 0.38\left(1 - e^{-2L_G}\right)} \tag{5}$$

Step 7: Calculate the vertical adjustment factor, $v_{0.01}$, for 0.01% of the time:

$$\zeta = \tan^{-1}\left(\frac{h_R - h_s}{L_G\,r_{0.01}}\right) \qquad \text{degrees}$$

For $\zeta > \theta$, $$L_R = \frac{L_G\,r_{0.01}}{\cos\theta} \qquad \text{km}$$

Else, $$L_R = \frac{(h_R - h_s)}{\sin\theta} \qquad \text{km}$$

If $|\varphi| < 36°$, $$\chi = 36 - |\varphi| \qquad \text{degrees}$$

Else, $$\chi = 0 \qquad \text{degrees}$$

$$\nu_{0.01} = \frac{1}{1 + \sqrt{\sin\theta}\left(31\left(1 - e^{-(\theta/(1+\chi))}\right)\frac{\sqrt{L_R\,\gamma_R}}{f^2} - 0.45\right)}$$

Step 8: The effective path length is:

$$L_E = L_R\,\nu_{0.01} \qquad \text{km} \tag{6}$$

Step 9: The predicted attenuation exceeded for 0.01% of an average year is obtained from:

$$A_{0.01} = \gamma_R\,L_E \qquad \text{dB} \tag{7}$$

Step 10: The estimated attenuation to be exceeded for other percentages of an average year, in the range 0.001% to 5%, is determined from the attenuation to be exceeded for 0.01% for an average year:

If $p \geq 1\%$ or $|\varphi| \geq 36°$: $\beta = 0$

If $p < 1\%$ and $|\varphi| < 36°$ and $\theta \geq 25°$: $\beta = -0.005(|\varphi| - 36)$

Otherwise: $\beta = -0.005(|\varphi| - 36) + 1.8 - 4.25\sin\theta$

$$A_p = A_{0.01}\left(\frac{p}{0.01}\right)^{-(0.655 + 0.033\ln(p) - 0.045\ln(A_{0.01}) - \beta(1-p)\sin\theta)} \qquad \text{dB} \tag{8}$$

This method provides an estimate of the long-term statistics of attenuation due to rain. When comparing measured statistics with the prediction, allowance should be given for the rather large year-to-year variability in rainfall rate statistics (see Recommendation ITU-R P.678).

2.2.1.2 Long-term frequency and polarization scaling of rain attenuation statistics

The method of § 2.2.1.1 may be used to investigate the dependence of attenuation statistics on elevation angle, polarization and frequency, and is therefore a useful general tool for scaling of attenuation according to these parameters.

If reliable attenuation data measured at one frequency are available, the following empirical formula giving an attenuation ratio directly as a function of frequency and attenuation may be applied for frequency scaling on the same path in the frequency range 7 to 55 GHz:

$$A_2 = A_1 \left(\varphi_2 / \varphi_1\right)^{1-H(\varphi_1, \varphi_2, A_1)} \tag{9}$$

where:

$$\varphi(f) = \frac{f^2}{1+10^{-4} f^2} \tag{10a}$$

$$H(\varphi_1, \varphi_2, A_1) = 1.12 \times 10^{-3} (\varphi_2 / \varphi_1)^{0.5} (\varphi_1 A_1)^{0.55} \tag{10b}$$

A_1 and A_2 are the equiprobable values of the excess rain attenuation at frequencies f_1 and f_2 (GHz), respectively.

Frequency scaling from reliable attenuation data is preferred, when applicable, rather than the prediction methods starting from rain data.

When polarization scaling is required, it is more appropriate to use directly the parameters k and α as given in Recommendation ITU-R P.838. These parameters also provide a radiometeorological basis for frequency scaling.